THE ANNUAL REPORT OF THE MSU GROUP

(Jan.-Dec. 2001)

Contributors: V.B.Braginsky (P.I.), I.A.Bilenko, M.L.Gorodetsky, F.Ya.Khalili, V.P.Mitrofanov, K.V.Tokmakov, S.P.Vyatchanin

The researches were supported by NSF grant #PHY98-00097 "Suspensions and suspension noise for LIGO test masses" (July 1998 – June 2001) and by NSF grant "Low noise suspensions and readout systems for LIGO" (July 2001 – June 2004)

Contents

I. SUMMARY

A. The improvement of violin modes Q-factors in fused silica suspension of the test mass

According to the list of tasks formulated in the program of this grant V.P.Mitrofanov and K.V.Tokmakov have carried out direct measurements of the Q-factors of violin modes in a suspension of the test mass model. Before this new test the highest obtained value of the Q was about 1×10^8 (see V.B.Braginsky et al., Physics-Doklady, 40 (1995) 11, S.Rowan et al, Proceeding of the Third Edoardo Amaldi Conference, AIP , Melville, NY, 2000). In these new tests special precautions were made to reduce the possible additional losses caused by sedimentation of fused silica vapour on the surface of the pin and the fiber during the welding (hydrofluoric acid was used to remove visible sedimentation). Another procedure was used in the new tests which allowed to reduce the second possible source of additional losses: the adsorbed and absorbed water. The fiber was baked during 6 hours at the temperature 260C inside the vacuum chamber by a special oven that was installed around the fiber. The net result of these tests was the rise of Q of the lowest violin mode up to $Q = 2.45 \times 10^8 (\pm 10\%)$. The expected value of Q in this test (based on the value of the intrinsic loss and on the dilution factor) would be $Q = (5 \div 10) \times 10^8$. It is necessary to note that in a similar test P.Willems at Caltech has reached recently the value $Q = 5 \times 10^8$.

The gap between these two values probably is due to not perfect (in MSU experiment) system of reduction of the recoil losses in the supporting elements of the installation and more perfect system of the fiber fabrication developed at Caltech.

B. Measurement of electric charges on the fused silica test masses

The second task formulated in the program of the grant is the measurement of dc and ac components of the electric charge on the mirror. These two components may mimic the action of gravitational wave on the mirror if an electrostatic actuator consists of a flat fused silica plate that is covered with two sets of metal stripes. If the surface of the mirror without coating has electric potential $U = 30V$ and the electric charge on it changes by $\Delta q = 8 \times 10^{-16}$C $\simeq 5 \times 10^3$ electrons then the "jump" of the Coulomb force acting on the mirror will be $F_c \simeq 3 \times 10^{-8}$ dyn for the actuator with the square area 10cm^2 and actuator-mirror gap $d = 0.2$cm. This value F_c is in the order of the amplitude of force corresponding to the action of gravitational wave in LIGO II ($h = 10^{-22}$, $m = 10^4$ g).

Two experiments were realized by V. Mitrofanov, K.Tokmakov and postgraduate student I.Elkin. In the first one the vibrating capacitor probe technique was used to measure the value of the electric charge on a fused silica plate situated in vacuum. In this experiment the level of the obtained sensitivity corresponds to variation of the charge density $\sigma \simeq 4 \times 10^{-17}$ C/cm^2 $\simeq 3 \times 10^2$ electrons/cm^2 (see details in: I.A.Elkin, V.P.Mitrofanov, Method of measurement of electrostatic charges on the surface of dielectric specimens, Moscow Univ. Phys. Bull., N5, (2001) 47). In the second experiment the electric charge on 0.5kg model of the fused silica mirror suspended by two silica fibers in the high vacuum chamber was measured. In this one the rise of the electric charge with a rate of about 2×10^{-12} C/cm^2 $\simeq 10^7$ electrons/cm^2 per two weeks was observed. At present these experiments continue.

C. The development and the improvement of methods of registration of small excess noise in the violin modes of all fused silica suspension

The task of measurements of small excess noise in the violin modes of fused silica fibers turn out to be a much more difficult one in comparison with the measurements of the same class of noise in steel and tungsten wires. During the last year a new readout system (after two preceding ones which failed to guarantee the necessary sensitivity) was tested. In this system a small diamond-shaped flat plate of fused silica covered with high reflective coating was welded into the middle of a fused silica fiber. After the welding direct tests have shown that the welding to the sharp corners of the plate does not damage the coating and the mechanical quality factor of the violin mode (the value of the obtained finesse is higher than

50). This value is sufficient to reach the sensitivity at level $\sim 5 \times 10^{-13}\mathrm{cm}/\sqrt{\mathrm{Hz}}$ with few milliwatts power from a He-Ne laser). Apart from this problem special precautions were used for not to ruin the high quality factor of the violin modes in the support structure and in the load. This will allow to decrease substantially the recoil losses and thus to save high Q factors of violin modes.

At present the process of assembling of all elements of the test installation is in progress.

D. The development of the method of measurement of thermorefractive noise in fused silica

M.L.Gorodetsky and his student I.S.Grudinin are finishing the assembling of new installation aimed to observe thermorefractive noise in fused silica microspheres and to test in this way predictions of this noise in LIGO antenna.

The installation is based on small chamber for the resonator which may either be evacuated or filled with pure nitrogen. In this chamber having optical windows, fused silica cantilever is installed for fine positioning of microspheres relative to coupling prism.

Nd:YAG diode pumped laser (Lightwave Electronics, 1.064μm) with narrow linewidth analogous to the lasers in LIGO antennas will be used for the measurements. In preliminary tests of microspheres (diameter $600 - 200\mu m$) in the chamber with this laser, optical modes with Q-factors of the order of (10^9) were observed with pronounced thermal nonlinearity.

The main difficulty in measurements should be stabilization of frequency of the laser on the slope of the resonant curve in presence of strong thermal nonlinearity. Computer based stabilization scheme is now in preparation.

Numerical simulation of thermal nonlinearity in microspheres is also in progress now aiming to find optimal methods for locking the laser on the mode with strong thermal nonlinearity. The modeling revealed regimes of oscillatory instability in microspheres which were experimentally observed but not explained several years ago in MSU group.

The theoretical calculations of spectral densities of this noise in microspheres were given in the previous annual report and presented at international symposium Photonics West'2001 in San-Jose and published in Proc. of SPIE **4270** (2001).

See in appendix D the theoretical analysis of the connection between thermorefractive noise and nonlinear response of the microresonator which may simplify the experimental verification.

E. The analysis of table-top quantum measurement with macroscopic masses

At the stage II of the LIGO project (years 2006-8) the antennae sensitivity is expected to be close to the Standard Quantum Limit, and in the stage III the sensitivity will have to be better.

The members of the MSU group share the point of view that before the implementation of any version of QND measurement in the LIGO project, apart from scrupulous analysis it will be fruitful to realize at table-top scale a real experiment with small test masses. This type of test may permit to discover undesirable effects which might be missed in the modeling. F.Ya.Khalili and his student P.S.Volikov carried out analysis of such a scheme.

The scheme of experiment is based on two concepts: the difference between the free test mass and the oscillator SQL sensitivity, and the use of mechanical rigidity produced by an optical pumping field in Fabry-Perot resonator to convert the free test mass into the mechanical oscillator having very low intrinsic noises. The analysis shows that proposed scheme allows to circumvent the free test mass Standard Quantum Limit by the factor $\xi \simeq 0.1$, using good, but not unique mirrors with $1 - R \simeq 10^{-5}$ (R is the reflectivity factor), and moderate pumping power $W \simeq 50$mWt.

The main goal of the proposed experiment will be to show that various noises of non quantum origin does not prevent to achieve sensitivity better than the SQL at room temperatures. Evidently there are others, more sophisticated schemes of measurements which may provide better sensitivity. At present there are two evident "candidates". In the first one (which is a simpler one) it is possible to use variational measurement by periodic modulation of the phase of the reference beam. The second one is the stroboscopic measurement which is in essence a Quantum Non-Demolition measurement of the probe oscillator quadrature amplitude (see details in the Appendix E).

F. Frequency-dependent rigidity in large-scale interferometric gravitational-wave detectors

Several methods to overcome the SQL has been proposed but most of them encounter serious technological limitation and/or has some other disadvantages which make implementation of these methods hard in the near future. On the other hand, the SQL itself is not an absolute limit but, in particular, it depends on the dynamic properties of the test object which is used in the experiment. The well known example is the harmonic oscillator, which allows to obtain sensitivity better than the SQL for the free mass when the signal frequency is close to the eigen frequency of the oscillator Ω_m.

F.Ya.Khalili has shown, that electromagnetic rigidity which exists in large-scale optical resonators if pumping frequency is detuned from the eigen frequency of resonator have sophisticated spectral dependence which allows to obtain sensitivity better than the SQLs both for the free test mass and the harmonic oscillator. Depending on the detuning, the bandwidth of the resonator and the pumping power, several regimes of this frequency-dependent rigidity are possible. In particular, the second-order-pole regime allows to "dive" deep below the SQL in the narrow spectral band $\Delta\Omega$ which is, however, much wider than if the usual frequency independent rigidity is used. It is important that the pumping energy in this regime does not depend on the sensitivity and remains approximately equal to the energy which is necessary to achieve the SQL in the traditional scheme of the interferometric position meter.

The third-order-pole regime provides sensitivity a few times better than the SQL in relatively wide spectral band and extremely low level of the measurement noise in this band. However its backaction noise is rather large. This regime looks as a good candidate for use in advanced topologies of the gravitational-wave antennae, based on use of separate optical modes for measurement and for creating rigidity, or/and which eliminate back-action noise by using variational measurement (see details in the Appendix F).

G. Parametric Oscillatory Instability in Fabry-Perot Resonator

S. P. Vyatchanin and his student S. E. Strigin have analyzed undesirable effect of parametric instability which (being ignored) may cause very substantial decrease of the antennae sensitivity and even may make the antenna unable to work properly. This effect is originated from the fact that in LIGO-II high value of optical energy $\mathcal{E}_0$ is planned to be stored in the Fabry-Perot resonator optical mode: $\mathcal{E}_0 > 30$ J (it corresponds to the circulating power W of the order 0.8 megawatt).

This effect takes place if mode of elastic oscillations in FP resonator mirrors with frequency ω_m and Stokes optical mode with frequency ω_1 are coupled with optical main mode with frequency ω_0 (which is pumped) by parametric condition $\omega_0 \simeq \omega_1 + \omega_m$. The origin of parametric instability can be described qualitatively in the following way: small mechanical oscillations with the resonance frequency ω_m modulate the distance L between mirrors that causes the excitation of optical fields with frequencies $\omega_0 \pm \omega_m$. Therefore, the Stokes mode amplitude will rise linearly in time if time interval is shorter than relaxation time of Stokes mode. The presence of two optical fields with frequencies ω_0 and ω_1 will produce the component of ponderomotive force (which is proportional to square of sum field) with difference frequency $\omega_0 - \omega_1$. Thus this force will increase the initially small amplitude of mechanical oscillations. It is obvious that at some threshold level of initial energy $\mathcal{E}_0$ in main mode this "feedback" prevails the damping in Stokes and elastic mode — it may give birth to the parametric oscillatory instability.

The calculations for simplified model shows that in resonance case parametric instability may take place when value of optical energy is about ~ 300 times smaller that planned in LIGO-II. Several recommendations to obtain a guarantee to evade this non-desirable effect and details of calculations are presented in Appendix G.

H. Collaboration of MSU group with group of K. S. Thorne

1. *Conversion of conventional gravitational-wave interferometers into QND interferometers*

This part of researches was done by S. P. Vyatchanin in collaboration with H.J.Kimble, Yuri Levin, Andrey B.Matsko and K.S.Thorne.

The possible designs for interferometers that can beat the SQL (LIGO-III) was analyzed. These designs are identical to a conventional broad-band interferometer (without signal recycling) except for new input and/or output optics. Three variants of design were analyzed:

1. A *squeezed-input interferometer* in which squeezed vacuum with frequency-dependent (FD) squeeze angle is injected into the interferometer's dark port.

2. A *variational-output* interferometer, in which homodyne detection with FD homodyne phase is performed on the output light;

3. A *squeezed-variational interferometer* with squeezed input and FD-homodyne output.

It is shown that the FD squeezed-input light can be produced by sending ordinary squeezed light through two successive Fabry-Perot filter cavities before injection into the interferometer, and FD-homodyne detection can be achieved by sending the output light through two filter cavities before ordinary homodyne detection. With anticipated technology (power squeeze factor $e^{-2R} = 0.1$ for input squeezed vacuum and net fractional loss of signal power in arm cavities and output optical train $\epsilon_* = 0.01$) and using an input laser power I_o in units of that required to reach the SQL (the planned LIGO-II power, $I_{\rm SQL}$), the three types of interferometer could beat the amplitude SQL at 100 Hz by the following amounts $\mu \equiv \sqrt{S_h}/\sqrt{S_h^{\rm SQL}}$ and with the following corresponding increase $\mathcal{V} = 1/\mu^3$ in the volume of the universe that can be searched for a given non-cosmological source:
Squeezed-Input — $\mu \simeq \sqrt{e^{-2R}} \simeq 0.3$ and $\mathcal{V} \simeq 1/0.3^3 \simeq 30$ using $I_o/I_{\rm SQL} = 1$.

Variational-Output — $\mu \simeq \epsilon_*^{1/4} \simeq 0.3$ and $\mathcal{V} \simeq 30$ but only if the optics can handle a ten times larger power: $I_o/I_{\rm SQL} \simeq 1/\sqrt{\epsilon_*} = 10$.

Squeezed-Variational — $\mu = 1.3(e^{-2R}\epsilon_*)^{1/4} \simeq 0.24$ and $\mathcal{V} \simeq 80$ using $I_o/I_{\rm SQL} = 1$; and $\mu \simeq (e^{-2R}\epsilon_*)^{1/4} \simeq 0.18$ and $\mathcal{V} \simeq 180$ using $I_o/I_{\rm SQL} = \sqrt{e^{-2R}/\epsilon_*} \simeq 3.2$.

The details see in LANL Archive (qr-qc/0008026). The paper is submitted to Phys. Rev. D.

2. Reducing of Thermoelastic Noise by Reshaping the Light Beams and Test Masses

This part of researches are being done by S. P. Vyatchanin and his student S. E. Strigin in collaboration with Erika D'Ambrosio, Richard O'Shaughnessy and Kip S.Thorne.

Thermoelastic fluctuations of mirror's surface decrease considerably if beam with larger radius is used. This source of noise is very significant in sapphire test masses (as it was shown in *Physics Letters A* **A264** (1999) 1). In order to decrease the thermoelastic fluctuations of mirrors surface it was proposed to use so called "Mexican-hat" light beam in the LIGO interferometers. These beams has larger radius of beam than Gaussian beams at the same difractional losses and hence thermoelastic noise for such beams is smaller. It was also proposed to use conic shape of test masses (instead of cylindric one). The preliminary results show that both these modifications allow to decrease thermoelastic noise by factor $4 \div 8$.

The article is in preparation (see also LIGO documents G010151-00 and G010297-00).

I. Collaboration of MSU group with LIGO team

In 2001 the fruitful collaboration between LIGO team and MSU group continued. V.Mitrofanov has visited Caltech and Phil Willems has visited MSU. Now P.Willems and V.Mitrofanov together with other colleagues prepare paper "Investigation of the Dynamics and Mechanical Dissipation of a Fused Silica Suspension" which describes the highest violin modes Q's yet measured in fused silica.

II. APPENDIXES

Appendix D. The development of the method of measurement of thermorefractive noise in fused silica

Thermodynamical fluctuations of temperature in the mirrors of LIGO are essential for the estimates of ultimate sensitivity of the antenna. These fluctuations lead to thermoelastic and thermorefractive noises due to effects of thermal expansion and thermal dependence of index of refraction.

Thermorefractive noise may be analysed in laboratory conditions using microspheres with whispering gallery modes. These microresonators combine very small effectiv volume (the diameter is of the order of $100\mu m$, and effectve volume is of the order of $10^{-8} cm^3$) with very high quality factor of optical modes ($\sim 10^9$).

For correct interpretation of measurements of thermorefractive noise spectral density in microspheres is complicated by the difficulties with precise identification of the excited mode and hence the uncertainty of the distribution of the optical field. One may show, however, that this spectral density may be verified and compared with the results of another independent and simpler measurement - nonlinear responce of resonance frequency on the weak modulation of input optical power.

The modulation of intensity in the mode leads to the modulation of the temperature of the mode volume and hence through the change of refraction index $\delta n = \frac{dn}{dT}\delta u$ to the change of resonance frequency. This effect is known as thermal nonlinearity and may be analysed using equation of temperature conductivity:

$$\frac{\partial u}{\partial t} - a^2 \Delta u = \frac{\omega W}{Q_a C \rho}$$

where $W = \frac{n^2|\vec{E}|^2}{8\pi}$ is internal energy density in the mode and $Q_a = 2\pi n/\alpha\lambda$ (α is absorption). $|\vec{E}|^2 = I(t)|\vec{E}_0|^2$, where $\int |\vec{E}_0|^2 d\vec{r} = 1$, C is specific heat capacity, and ρ is density of the material of the microresonator.

In spectral form we obtain:

$$u(\Omega,\vec{r}) = \gamma I(\Omega)\int \frac{G(\vec{\beta})e^{i\vec{\beta}\vec{r}}}{a^2\beta^2 + i\Omega}\frac{d\vec{\beta}}{(2\pi)^3}$$

where

$$\gamma = \frac{\alpha n c}{8\pi C\rho}$$
$$G(\vec{\beta}) = \int |\vec{E}_0|^2 e^{-i\vec{\beta}\vec{r}} d\vec{r}$$

is the spacial spectrum of energy distribution of the mode. Averaging temperature over the mode volume we obtain the spectrum of temperature modulation:

$$\begin{aligned}\bar{u}(\Omega) &= \int u|\vec{E}_0|^2 d\vec{r} = \gamma I(\Omega)\int\int\int \frac{|\vec{E}_0(\vec{r})|^2|\vec{E}_0(\vec{r}')|^2 e^{i\vec{\beta}(\vec{r}-\vec{r}')}}{a^2\beta^2 + i\Omega} d\vec{r}\, d\vec{r}'\, \frac{d\vec{\beta}}{(2\pi)^3} \\ &= \gamma I(\Omega)\int \frac{|G(\vec{\beta})|^2}{a^2\beta^2 + i\Omega}\frac{d\vec{\beta}}{(2\pi)^3} \\ &= \gamma I(\Omega)\left[a^2\int \frac{\beta^2|G(\vec{\beta})|^2}{a^4\beta^4 + \Omega^2}\frac{d\vec{\beta}}{(2\pi)^3} + i\Omega\int \frac{|G(\vec{\beta})|^2}{a^4\beta^4 + \Omega^2}\frac{d\vec{\beta}}{(2\pi)^3}\right] \qquad (1)\end{aligned}$$

This is the responce of the temperature on intensity modulation that may be measured by measuring the dependence of resonance frequency modulation $\frac{\delta\omega}{\omega}(\Omega) = \frac{1}{n}\frac{dn}{dT}\delta u(\Omega)$ from the modulation of input power.

From the other hand the spectral density of thermodynamical fluctuations of temperature. averaged over the mode volume mayt be found see the papers as:

$$\bar{u} = \int u(\vec{r},t)|E_0(\vec{r})|^2 d\vec{r},$$

where

$$u(\vec{r},t) = \int \frac{F(\vec{\beta},\Omega)}{a^2\beta^2 + i\Omega} e^{i\Omega t + i\vec{\beta}\vec{r}} \frac{d\Omega\, d\vec{\beta}}{(2\pi)^4}$$
$$< F(\vec{\beta}',\Omega')F^*(\vec{\beta},\Omega) >= \frac{2a^2kT^2}{\rho C}\beta^2\delta(\beta-\beta')\delta(\Omega-\Omega')$$

(see our previous report or *Physics Letters A*, **A264** (1999) 1)

Hence

$$S_{\bar{u}}^2 = \frac{2a^2kT^2}{\rho C}\int\int\int \frac{\beta^2}{a^4\beta^4+\Omega^2}|E_0(\vec{r})|^2|E_0(\vec{r}')|^2 e^{i\vec{\beta}(\vec{r}-\vec{r}')}drdr'\frac{d\vec{\beta}}{(2\pi)^3}$$
$$= \frac{2kT^2}{\rho C}a^2\int \frac{\beta^2|G(\vec{\beta})|^2}{a^4\beta^4+\Omega^2}\frac{d\vec{\beta}}{(2\pi)^3} \qquad (2)$$

Now comparing this result with (1) we find

$$S_u^2 = \frac{16\pi kT^2}{\alpha nc}\frac{\Re u(\Omega)}{I(\Omega)}$$

This equation gives connection between nonlinear responce and spectral density of noise which is somewhat analogous to flutuation-dissipation theorem.

Appendix E. The analysis of table-top quantum measurement with macroscopic masses

Introduction

There is an evident steady progress in improvement of the sensitivity in many types of physical measurements. Particularly, in the previous century late 80-s several groups of experimentalists successfully demonstrated the resolution better than the Standard Quantum Limit (SQL) in optical domain using QND methods (e.g. see review article [1]). At the end of the 90-s even more impressive experiment was realized in the microwave domain. In this experiment single microwave quanta were counted without absorption [2]. At the same time experiments with resolution better than SQL using mechanical test objects are not yet realized.

There is at least one area in the experimental physics where the necessity to circumvent the SQL of sensitivity using mechanical test masses is crucially important. This is the terrestrial gravitational wave antennae creation. At the stage II of the LIGO project (years 2006-8) the antennae sensitivity is expected to be close to the SQL, and in the stage III the sensitivity will have to be better [3]. There were several articles with different schemes of measuring devices aimed to "beat" the SQL for mechanical objects (see, for example, articles [4], [5], [6], [7]. In the majority of these articles only concepts of new methods were presented and only one of them [7] has provided rather detailed analysis of the measurement scheme using mechanical object (mirror of the gravitational-wave antenna) based on QND principle. It was shown that proposed scheme can be implemented provided that very sophisticated cryogenic technique is used.

In this article we present the analysis key parts for a simple experiment scheme using relatively small test masses that is able to provide the sensitivity better than the free test mass SQL and can be realized in relatively modest laboratory conditions.

The first initial principle of the scheme is based on the difference between the sensitivity

SQLs for the force F acting on the free mass m and mechanical oscillator having the same mass and eigenfrequency Ω_m:

$$F_{\rm SQL}^{\rm free\,mass} \simeq \sqrt{\frac{\hbar m \Omega_F^2}{\tau}}\,, \tag{3}$$

$$F_{\rm SQL}^{\rm oscillator} \simeq \frac{\sqrt{\hbar m \Omega_F}}{\tau}\,, \tag{4}$$

where Ω_F is the mean frequency of the force and τ is its duration. These equations are valid if $\tau \gtrsim 1/\Omega_F$ and $|\Omega_F - \Omega_m| \lesssim 1/\tau$.

Comparing equations (3) and (4) one may conclude that it is possible to "beat" the *free mass* SQL by the factor

$$\xi = \frac{F_{\rm SQL}^{\rm oscillator}}{F_{\rm SQL}^{\rm free\,mass}} \simeq \left(\frac{1}{\Omega_F \tau}\right)^{1/2}, \tag{5}$$

using test mass with sufficiently low noise rigidity $m\Omega_m^2$ attached to it. It can be shown (see Appendix II) that the exact form of this condition is

$$\xi = \left(\frac{\Delta\Omega}{\Omega_F}\right)^{1/2}, \tag{6}$$

where $\Delta\Omega \simeq 1/\tau$ is the bandwidth of the force.

The second initial principle of the scheme is based on the possibility to create mechanical rigidity provided by the dependence of light pressure on the detuned Fabry-Perot resonator mirrors position. We have already analyzed the possibility to create very low noise rigidity using the pumping frequency ω_p detuned much far from the resonator eigenfrequency ω_o [8]. It was supposed in article [8] that separate resonator must be used as a measuring device.

In this article we propose another simpler scheme where the same resonator serves as the meter and the rigidity source. In this case optimal detuning $\delta = \omega_p - \omega_o$ should be close to the resonator semi-bandwidth $\gamma = \omega_o/2Q_{\rm FP}$, where $Q_{\rm FP}$ is the quality factor of the resonator. We show that this scheme allows to reach the limiting value ξ [see formula (6)].

We have to note that the potential possibilities to use the mechanical rigidity of optical origin in different LIGO readout meters were already discussed in [9], [10]. These possibilities are indicating that SQL can be circumvented in narrow bandwidth. In the presented below analysis we were trying to give answers to most important practical issues which may appear in the implementation of such an experiment.

The main elements of the design and the experiment scheme

The test mass suspension The most important elements of the experimental setup are the test mass suspension, optical rigidity, and optical readout scheme. Simplified sketch of experimental scheme is presented on Fig.1.

The necessary condition for such kind of experiments is a sufficiently low dissipation in the suspension. The quality factor of the mechanical test oscillator has to exceed value

$$Q_m \gtrsim \frac{2\kappa T}{\hbar\Omega_F\xi^2} \simeq \frac{10^{10}}{\xi^2}\times\left(\frac{T}{300\mathrm{K}}\right)\times\left(\frac{10^4\,\mathrm{s}^{-1}}{\Omega_F}\right), \tag{7}$$

where κ is the Boltzmann constant, and T is the heatbath temperature. In fact, this inequality represents the condition that the fluctuating force originated from mechanical losses in the suspension (according to FDT) has to be ξ^{-1} times smaller than the force $F_{\rm SQL}^{\rm free\, mass}$.

The estimate (7) show that an ordinary mechanical spring can't be used here. It is necessary to use "artificial" rigidity with very low intrinsic noises, and optical ponderomotive rigidity does look promising. In this case the suspension can be similar to the Galileo pendulum with eigenfrequency $\Omega_{\rm pend} \ll \Omega_F$. The relaxation time of $\tau^*_{\rm pend} \simeq 2\times 10^8$s has been already obtained for all fused silica suspension of the LIGO mirror model. This value of $\tau^*_{\rm pend}$ allows in principle to obtain the quality factor of $Q_m \simeq \Omega_m\tau^*_{\rm pend} \simeq 2\times 10^{12}$ (even if the viscous model of friction is valid) and thus allows to reach $\xi \simeq 0.1$. In the Appendix c more rigorous analysis of the suspension noises is presented, which shows that these noises do not prevent from obtaining the sensitivity of $\xi \lesssim 0.1$.

It is evident that the platform the suspending fiber has to be welded to must be a compact one: the mechanical eigenmodes of the platform have to be substantially higher than the chosen value of Ω_F. If the value $m \simeq 2 \times 10^{-2}$g (a few millimeters in dimension cylinder covered with high-reflectivity multilayer coating) then for $\Omega_F \simeq 10^4\text{s}^{-1}$ the meter has to register the oscillations of the mass with the amplitude of

$$\Delta x = \sqrt{\frac{\hbar}{m\Omega_F}} \simeq 2 \times 10^{-15}\text{cm}\,.$$

We omit here calculations which show that if the platform has sizes of a few centimeters and is manufactured from fused silica then quality factor of the eigenmodes that is higher than 10^5 will be sufficient to register this value of Δx.

It seems appropriate to use the first mirror of the Fabry-Perot resonator M1 as the test mass and the second mirror M2 must be attached rigidly to the platform (see Fig.1).

The optical rigidity It is a relatively easy task to "convert" the mass $m \simeq 2\times 10^{-2}$g into a mechanical oscillator with eigenfrequency $\Omega_m \simeq 10^4\text{s}^{-1}$. If the mass is the Fabry-Perot resonator mirror (see Fig. 1) and the laser is tuned on the one of the resonator resonance curves slope then the rigidity will be equal to

$$m\Omega_m^2 = \frac{16\omega_o W\mathcal{F}^2}{\pi^2 c^2}\frac{\delta/\gamma}{\left[1+(\delta/\gamma)^2\right]^2} \simeq 2\times 10^6\text{dyn/cm} \times \left(\frac{W}{50\text{mW}}\right) \times \left(\frac{\mathcal{F}}{10^3}\right)^2 \times \frac{\delta/\gamma}{\left[1+(\delta/\gamma)^2\right]^2}\,. \tag{8}$$

where $\omega_o = 2 \times 10^{15}\text{s}^{-1}$ is the optical pumping frequency, $\mathcal{F}$ is the finesse of the optical resonator, W is the pumping power.

Fig.2 illustrates the dependence of the laser ponderomotive force on the distance between the mirrors. Dashed line corresponds to the pendulum rigidity $m\Omega_{\text{pend}}^2$. There is a relatively big number n of static equilibrium points (which correspond to the crossings of the right slopes of the resonant curves with the horizontal axis; these points are marked by Xs on the Fig.2):

$$n = \frac{4\omega_o W\mathcal{F}}{\pi^2 m c^3 \Omega_{\rm pend}^2} \simeq 500 \times \left(\frac{W}{50{\rm mW}}\right) \times \left(\frac{\mathcal{F}}{10^3}\right) \times \left(\frac{10{\rm s}^{-1}}{\Omega_{\rm pend}}\right)^2 . \tag{9}$$

Thus by choosing one of these points experimentalists may change the rigidity. Another way for changing it is to apply a d.c. force onto the mirror (using for example the light pressure from another laser).

This rigidity has one disadvantage: it is associated with negative friction which corresponds to the characteristic time ("negative relaxation time") equal to

$$\tau_{\rm instab} = \frac{\gamma}{2\Omega_m^2}\left[1 + (\delta/\gamma)^2\right] . \tag{10}$$

If the finesse of the resonator is $\mathcal{F} \simeq 10^3$ and its length is $L \lesssim 1{\rm cm}$ then $\gamma \gtrsim 5 \times 10^7{\rm s}^{-1}$, and the value of $\tau_{\rm instab}$ can be large enough to provide sufficient time for the measurement, $\Omega_m \tau_{\rm instab} \gtrsim 10^4$.

The optical readout scheme The optical readout scheme is presented on the left part of the Fig.1 The pumping laser beam is splitted into two beams (the signal beam and the reference one). The signal beam enters the Fabry-Perot resonator and passes back carrying information about the displacement of the mirror M1 relative to M2 in its phase. The reflected beam is separated from the input one by polarization beam splitter PBS and Faraday isolator FI, and then is combined with the reference beam on the beamsplitter BS2. This beamsplitter together with photodetectors D1 and D2 form standard balanced homodyne detector. It is assumed that an arbitrary phase shift $\phi_{\rm LO}$ can be added to the reference beam.

The difference between the photocurrents in such a scheme depends on the phase shift of the signal beam relative to the reference one,

$$I_1 - I_2 = \frac{2e\sqrt{WW_{\rm ref}}}{\hbar\omega_o} \cos\left(\phi_1 + \frac{2\gamma\omega_o}{\gamma^2+\delta^2}\frac{x}{L} - \phi_2 - \phi_{\rm LO}\right)$$

and thus provides information about x. Here $W_{\rm ref}$ is the reference beams power, ϕ_1, ϕ_2 are the initial phases of the signal and reference beams.

It can be shown (see Appendix II) that if the Fabry-Perot resonator bandwidth is defined by the nonzero transmittance of the mirror M1 only, if there are no losses in all optical elements which the signal beam passed through, if quantum efficiency of the photodetectors are equal to unity and quantum state of the pumping beam is pure coherent one then the value (6) can be achieved in this ideal case.

In more realistic case when the above conditions are not fulfilled the total achievable value of ξ^2 is a sum of two terms: the "ideal" value described by formula (6) and additional value $\xi^2_{\rm optics}$ which depends on the parameters of the optical scheme. General expression for $\xi^2_{\rm optics}$ is very cumbersome. In asymptotic case when $\Delta\Omega/\Omega_F \ll 1$, losses are small and sufficiently large value of the pumping power can be provided, the value of $\xi^2_{\rm optics}$ can be presented as

$$\xi^2_{\rm optics} \approx \frac{1}{\sqrt{P}}\,\frac{1+(\delta/\gamma)^2}{(\delta/\gamma)^{3/2}} + \frac{\mathcal{A}}{\delta/\gamma}\,, \tag{11}$$

where P is a dimensionless parameter proportional to the pumping power:

$$P = \frac{64\omega_o W}{mc^2\Omega_F^2(1-\mathcal{R}_2)^2} \approx 1.5\times 10^4 \times \left(\frac{W}{50\text{mW}}\right) \times \left(\frac{20\text{mg}}{m}\right) \times \left(\frac{5\times 10^{-5}}{1-\mathcal{R}_2}\right)^2 \times \left(\frac{10^4\text{s}^{-1}}{\Omega_F}\right)^2, \tag{12}$$

$\mathcal{R}_2$ is the mirror M2 reflectivity,

$$\mathcal{A} = 1-\eta_{\rm PD}(1-\mathcal{A}_0)(1-\mathcal{A}_1) \approx 1-\eta_{\rm PD}+\mathcal{A}_0+\mathcal{A}_1 \tag{13}$$

is total "external losses", $\eta_{\rm PD}$ is quantum efficiency of the photodetectors, $\mathcal{A}_0$ is total absorption factor of the optical elements between the Fabry-Perot resonator and the photodetectors, $\mathcal{A}_1$ is the mirror M1 absorption factor. Expression (11) is valid if $P \gg 1$ and $\mathcal{A} \ll 1$.

It is evident that the sensitivity depends on the detuning δ. Optimal value of δ depends on whether first or second term prevails in the expression (11). If $\mathcal{A} \ll 1/\sqrt{P}$ then the optimal value is $\delta = \sqrt{3}\gamma$ and

$$\xi^2_{\rm optics} = \frac{4}{\sqrt{3\sqrt{3}P}} \approx \frac{1.75}{\sqrt{P}}\,. \tag{14}$$

In the opposite case the detuning must be large, $\delta/\gamma = (4\mathcal{A}^2 P)^{1/3} \gg 1$ and in this case

$$\xi^2_{\rm optics} = \frac{3}{2}\left(\frac{\mathcal{A}}{P}\right)^{1/3}\,. \tag{15}$$

These estimates show that even in the case of moderate conditions for the optical elements parameters losses in them don't prevent from obtaining the value of $\xi_{\rm optics} \simeq 0.1$ when the pumping power is sufficiently large, *e.g.* $W \gtrsim 50$mW.

If such a value of pumping power can't be provided then, nevertheless, the sensitivity slightly better than the SQL can be obtained, i.e. $\xi_{\rm optics} \simeq 0.3 \div 0.5$. Sensitivity for this case is calculated numerically. The results for the case when $\Delta\Omega/\Omega = 0.01$ are presented on the Fig.3 (solid line). Dashed line is the asymptote (32).

Conclusion

The scheme of measurement presented above may be regarded only as the first step along the route of "divine quantum" measurements with macroscopic quantum objects. The main goal of the proposed experiment will be to show that various noises of nonquantum origin do not prevent to achieve sensitivity better than the SQL even at room temperatures. Evidently there are others, more sophisticated schemes of measurements which may provide better sensitivity. At present there are two evident "candidates". In the first one (which is the simplier one) it is possible to use variational measurement [6] by periodic modulation of the phase of the reference beam $\phi_{\rm LO}$. The second one is the stroboscopic measurement [5] which is in essence a Quantum Non-Demolition measurement of the probe oscillator quadrature amplitude. In the second case it will be necessary to use two pumping lasers: the first one has to be permanently on and it will provide the rigidity, and the second one has to be turned on periodically during the time interval much shorter than Ω_m^{-1}.

The authors of this article have no doubts that the sensitivity better than the SQL may be obtained at the present level of experimental "culture" in the measurement with mechanical object.

Acknowledgments

This paper was supported in part by the California Institute of Technology, US National Science Foundation, by the Russian Foundation for Fundamental Research grants #96-02-16319a, #97-02-0421g and #99-02-18366-q, and the Russian Ministry of Science and Technology.

FIGURES

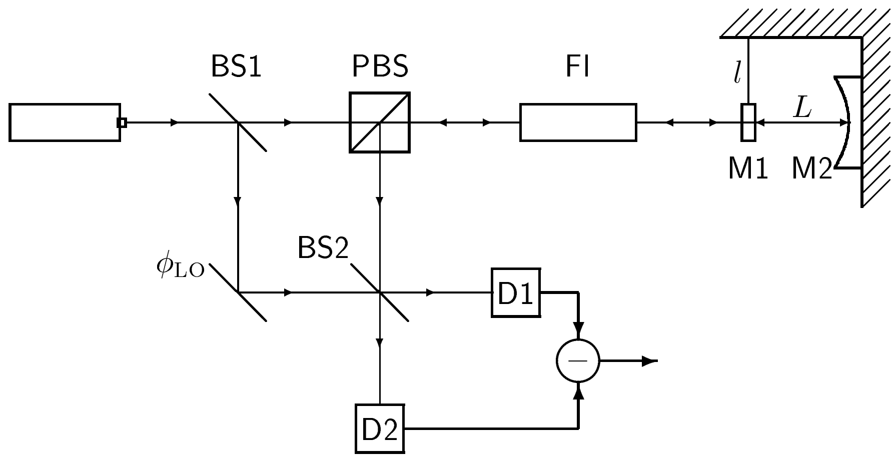

FIG. 1. Sketch of the experimental scheme

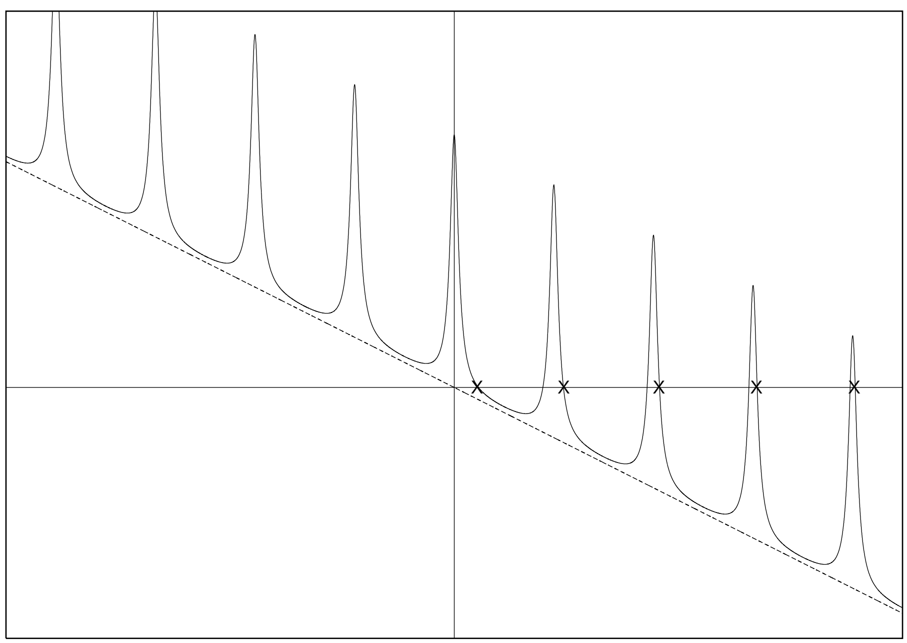

FIG. 2. Dependence of the ponderomotive force on the distance between the mirrors

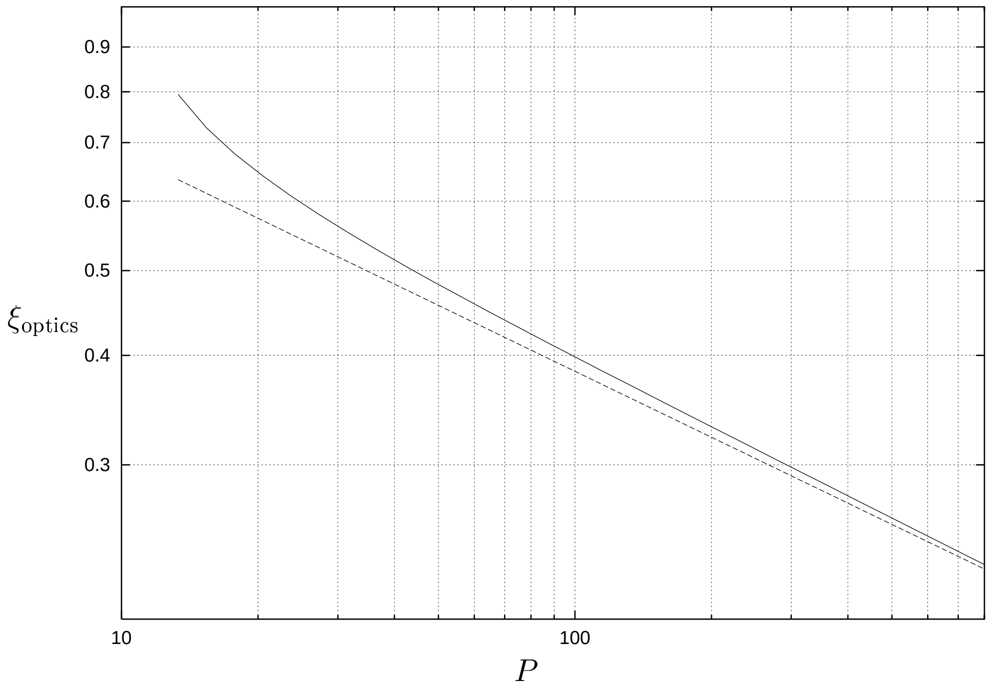

FIG. 3. Sensitivity as a function of the pumping power

Appendix A. The Standard Quantum Limits for the free mass and the oscillator

Total net noise of linear scheme for detection of classical force acting on the free test mass m is equal to [12]

$$F_{\text{free mass}}(t) = m\frac{d^2}{dt^2}x_{\text{fluct}}(t) + F_{\text{fluct}}(t)\,. \tag{16}$$

where $x_{\text{fluct}}(t)$ is the additive noise of the meter and $F_{\text{fluct}}(t)$ is its back-action noise.

For an ordinary position meter which sensitivity is limited by the SQL, these two noises are non-correlated and have frequency-independent spectral densities S_x and S_F, correspondingly, which satisfy the uncertainty relation

$$S_xS_F \geq \frac{\hbar^2}{4}\,. \tag{17}$$

We will suppose that noises are as small as possible and exact equality takes place in this formula.

In this case spectral density of the total noise (16) is equal to

$$S_{\text{free mass}}(\Omega) = m^2\Omega^4 S_x + S_F\,. \tag{18}$$

For any given observation frequency $\Omega = \Omega_F$ this value can be minimized by adjusting the ratio of the spectral densities $S_F/S_x = m^2\Omega_F^4$, giving

$$S^{\text{SQL}}_{\text{free mass}}(\Omega_0) = \hbar m \Omega_0^2. \tag{19}$$

This is the spectral form of the SQL for a free test mass [7].

In the case of an oscillator total net noise is equal to

$$F_{\text{oscillator}}(t) = \left(m\frac{d^2}{dt^2} + \Omega_0^2\right) x_{\text{fluct}}(t) + F_{\text{fluct}}(t)\,, \tag{20}$$

and its spectral density is equal to

$$S_{\text{oscillator}}(\Omega) = m^2(\Omega_0^2 - \Omega^2)^2 S_x + S_F\,. \tag{21}$$

By adjusting the ratio S_F/S_x in order to provide minimum of the spectral density at the edges of the narrow vicinity of the eigenfrequency Ω_0, $\Omega = \Omega_0 \pm \Delta\Omega/2$, where $\Delta\Omega \ll \Omega_0$, we obtain:

$$S^{\text{SQL}}_{\text{oscillator}}(\Omega_0 \pm \Delta\Omega/2) = \hbar m \Omega_0 \Delta\Omega\,. \tag{22}$$

The ratio of the spectral densities (19) and (22) is equal to (6).

Appendix B. The sensitivity limitation due to optical losses

a. Spectral density of the total net noise We will suppose that the Fabry-Perot resonator bandwidth is much larger than the observation frequency. It can be shown (we omit lengthy but quite straightforward calculations) that in the case of the Fabry-Perot position meter spectral densities S_x and S_F of the noises $x_{\rm fluct}$ and $F_{\rm fluct}$ introduced in the previous Appendix and their cross spectral density are equal to

$$S_x = \frac{\hbar}{2m\Lambda^2}\frac{1+(\delta/\gamma)^2}{\eta\sin^2\phi_{\rm LO}}, \qquad S_F = \frac{\hbar m\Lambda^2}{2}\frac{1}{1+(\delta/\gamma)^2}, \qquad S_{xF} = \frac{\hbar}{2}\cot\phi_{\rm LO}\,, \tag{23}$$

and the electromagnetic rigidity is equal to

$$\mathcal{K} = m\Omega_0^2 = \frac{m\Lambda^2}{2}\frac{\delta/\gamma}{1+(\delta/\gamma)^2} = \frac{4\omega_o\gamma_1(1-\mathcal{A}_1)W}{L^2\gamma^3}\;\frac{\delta/\gamma}{\left[1+(\delta/\gamma)^2\right]^2}\,, \tag{24}$$

where

$$\Lambda^2 = \frac{4\omega_o\mathcal{E}}{mL^2\gamma}\,, \qquad \eta = \frac{\gamma_1}{\gamma}(1-\mathcal{A})\,, \qquad \gamma_{1,2} = \frac{1-\mathcal{R}_{1,2}}{4L/c} \qquad (\gamma_1+\gamma_2=\gamma)\,, \tag{25}$$

$\mathcal{E}$ is pumping energy in the resonator, $\mathcal{R}_1, \mathcal{R}_2$ are the mirrors M1, M2 reflectivities, $\mathcal{A}$ is total "external losses" [see formula (13)].

Spectral density of the total noise of the meter in this case is equal to

$$S(\Omega) = \frac{\hbar m}{2}\left\{\frac{(\Omega^2-\Omega_F^2)^2\left[1+(\delta/\gamma)^2\right]}{\Lambda^2\eta\sin^2\phi_{\rm LO}} + \frac{1-\eta\cos^2\phi_{\rm LO}}{1+(\delta/\gamma)^2}\Lambda^2\right\}. \tag{26}$$

where

$$\Omega_F^2 = \Omega_0^2 - \frac{1}{2}\,\frac{\Lambda^2\eta\sin 2\phi_{LO}}{1+(\delta/\gamma)^2} = \frac{4\omega_o\gamma_1(1-\mathcal{A}_1)W}{mL^2\gamma^3}\;\frac{\delta/\gamma-\eta\sin 2\phi_{\rm LO}}{\left[1+(\delta/\gamma)^2\right]^2}\,. \tag{27}$$

b. Large pumping power Now our goal is to minimize the expression

$$\xi^2 \equiv \frac{S(\Omega_F \pm \Delta\Omega/2)}{\hbar m \omega_F^2} = \frac{(\Delta\Omega)^2\left[1+(\delta/\gamma)^2\right]}{2\Lambda^2\eta\sin^2\phi_{\rm LO}} + \frac{1-\eta\cos^2\phi_{\rm LO}}{\delta/\gamma - \eta\sin 2\phi_{\rm LO}}\,. \qquad (28)$$

It is evident that in order to obtain $\xi \ll 1$ it is necessary to have $\Delta\Omega/\Omega_F \ll 1$, $1-\eta \ll 1$ and $|\phi_{\rm LO}| \ll 1$. Taking it into account one can show that the expression (28) is minimal if

$$\phi_{\rm LO} = \phi_{\rm LO}^{\rm opt} \approx -\sqrt{\frac{\Delta\Omega}{\Omega_F}\,\frac{\delta/\gamma}{2}}\,, \qquad (29)$$

and the minimum is equal to

$$\xi^2 \approx \frac{\Delta\Omega}{\Omega_F} + \frac{\gamma_2/\gamma + \mathcal{A}}{\delta/\gamma}\left(1+\frac{2\phi_{\rm LO}^{\rm opt}}{\delta/\gamma}\right)\,. \qquad (30)$$

From this expression it is evident that the larger is the ratio δ/γ the smaller is ξ. On the other hand, the larger is this ratio the larger is the pumping power required to provide given $\Omega_F \approx \Omega_0$, see formula (24). If $\mathcal{A}_1 \ll 1$ and $\gamma_2 \ll \gamma_1$ then from (27) it follows that

$$\gamma \approx \sqrt{\frac{4\omega_o W}{mL^2\Omega_F^2}}\,\frac{\sqrt{\delta/\gamma}}{1+(\delta/\gamma)^2}\left(1-\frac{\phi_{\rm LO}^{\rm opt}}{\delta/\gamma}\right)\,. \qquad (31)$$

Substitution of this expression into formula (30) gives that

$$\xi^2 \approx \frac{\Delta\Omega}{\Omega_F} + \frac{1}{\sqrt{P}}\,\frac{1+(\delta/\gamma)^2}{(\delta/\gamma)^{3/2}}\left(1+\frac{3\phi_{\rm LO}^{\rm opt}}{\delta/\gamma}\right) + \frac{\mathcal{A}}{\delta/\gamma}\left(1+\frac{2\phi_{\rm LO}^{\rm opt}}{\delta/\gamma}\right)\,, \qquad (32)$$

Omitting here small terms proportional to $\phi_{\rm LO}^{\rm opt}$ we obtain formula (11).

c. Small pumping power If $P \simeq 1$ then it is possible to neglect the second term in the formula (11) because any good optical components can provide the value $\mathcal{A} \lesssim 0.1$. In this case it is necessary to minimize expression (28) with respect to $\phi_{\rm LO}$, γ_1 and δ with given values of the W and γ_2 and with additional condition (27). This minimization was performed numerically. Results are presented on the Fig.3.

We will base our consideration on the formula (11) in the article [13]. If the observation frequency Ω_F satisfies condition $\Omega_{\rm pend} \ll \Omega_F \ll \Omega_{\rm v}$, where $\Omega_{\rm v}$ is the eigenfrequency of the suspension fiber fundamental violin mode then this formula can be rewritten as:

$$S_x^{\rm susp} = \frac{4\kappa T}{I^2\Omega_F^6 l^2}\left\{\left[\frac{I}{m} - Rh\right]^2\zeta_{\rm top} + \left[\frac{I}{m} - (R+l)h\right]^2\zeta_{\rm bot}\right\}, \qquad (33)$$

where l is the length of the suspension fiber, I is the test-mass moment of inertia for rotation about the center of masses, R is the radius of the mirror face, m is the mass of the test mirror, h is the displacement of the laser beam spot from the center of the mirror, $\zeta_{\rm top}, \zeta_{\rm bot}$ are values characterizing dissipation at the top and the bottom of the fiber. Following authors of the article [13] we suppose that

$$\zeta_{\rm top} = \zeta_{\rm bot} = \zeta = \frac{\Omega_F\phi\sqrt{YJmg}}{2}, \qquad (34)$$

where Y is the Young modulus of the fiber material and $J = S^2/4\pi$ is the fiber geometrical momentum of inertia. If h is chosen optimally:

$$h = \frac{2R+1}{R^2+(R+l)^2}\cdot\frac{I}{M} \approx \frac{I}{Ml} \qquad (35)$$

then (we suppose that $R \ll l$)

$$S_x^{\rm susp} = \frac{4\kappa T\zeta}{m^2\Omega_F^6[R^2+(R+l)^2]} \approx \frac{4\kappa T\zeta}{m^2\Omega_F^6 l^2} \qquad (36)$$

This value of S_x corresponds to the spectral density of the fluctuating force acting on the test mass

$$S_{\rm susp} = m^2\Omega_F^4 S_x^{\rm susp} = \frac{4\kappa T\zeta}{\Omega_F^2 l^2} = \frac{2\kappa T\phi\sqrt{YJmg}}{\Omega_F l^2}. \qquad (37)$$

So the value of ξ^2 limited by the suspension noise is equal to

$$\xi^2_{\rm susp} = \frac{S_{\rm susp}}{\hbar m \Omega_F^2} = \frac{2\kappa T \phi}{\hbar \Omega_F^3 l^2}\sqrt{\frac{YJg}{m}} = \frac{\kappa T g}{\pi^2 \hbar v_o^2}\, \frac{\phi r \Omega_{\rm v}^2}{\mu^{3/2}\Omega_F^3}\,, \qquad (38)$$

where $v_o = \sqrt{Y/\rho}$ is the speed of sound in the fiber material, $\mu = \dfrac{mg}{YS}$ is dimensionless stress factor of the fiber.

For the room temperature and fused silica it will be

$$\xi^2_{\rm susp} \approx 4\times 10^{-4} \times \left(\frac{\phi r}{10^{-8}\,{\rm dyn/cm}}\right) \times \left(\frac{10^4\,{\rm s}^{-1}}{\Omega_F}\right) \times \left(\frac{\Omega_{\rm v}}{\Omega_F}\right)^2 \times \left(\frac{10^{-3}}{\mu}\right)^{3/2} \qquad (39)$$

Taking into account that values $\phi r \lesssim 10^{-8}$dyn/cm has been already obtained experimentally [14,15] it is possible to conclude that suspension noises don't prevent from obtaining the sensitivity $\xi \lesssim 0.1$.

REFERENCES

[1] P.Grangier, J.A.Levenson and J.-P.Poizat, Nature **396** (537) 1998

[2] G.Nogues *et al*, Nature **400** (239) 1999

[3] Proceedings of Third Edoardo Amaldi Conference, ed. by Sydney Meshkov, 1999

[4] C.M.Caves *et al*, Review of Modern Physics **52** 341 (1980)

[5] V.B.Braginsky, Yu.I.Vorontsov, F.Ya.Khalili, Sov. Phys. JETP Lett. **27** (1978) 276

[6] S.P.Vyatchanin, Physycs Letters **A239** (1998) 201.

[7] V.B.Braginsky, M.L.Gorodetsky, F.Ya.Khalili and K.S.Thorne, Physical Review **D61** (2000) 044002

[8] V.B.Braginsky, F.Ya.Khalili, Physics Letters A 257 (1999) 241

[9] F.Ya.Khalili, "Quantum experiments with macroscopic mechanical objects", proceedings of ICQO, Minsk, 2000 (in press)

[10] A.Buonanno, Y.Chen, "Quantum noise in second generation, signal-recycled laser interferometric gravitational-wave detectors", Phys.Rev.D (in press)

[11] V.B.Braginsky, V.P.Mitrofanov, K.V.Tokmakov, Physics Letters **A218** (1996) 164

[12] V.B.Braginsky, F.Ya.Khalili, *Quantum Measurement*, ed. by K.S.Thorne, Cambridge Univ. Press, 1992.

[13] V.B.Braginsky, Yu.Levin, S.P.Vyatchanin, Meas. Sci. Technol **10** (1999) 598

[14] V.P.Mitrofanov, O.I.Ponomareva, Vestnik Moskovskogo Universiteta, series 3, #5 (1987) 28

[15] S.D.Penn, G.M.Harry, A.M.Gretarsson, S.E.Kittelberger, P.R.Saulson, J.J.Schiller, J.R.Smith, S.O.Swords, Syracuse Univ. Gravitational Physics Preprint 2000/8-11

Appendix F. Frequency-dependent rigidity in large-scale interferometric gravitational-wave detectors

Introduction

The standard quantum limit (SQL) [1] is one of the most fundamental factors which prevent the gravitational-wave antennae [2] sensitivity from increasing. The basis for this limit is the uncertainty relation for two kind of noises inherent in position meters: the measurement noise and the back action noise. In the interferometric position meters, these noises are proportional to phase fluctuations of the pumping beam and radiation pressure noise, correspondingly.

Several methods to overcome the SQL has been proposed (see, for example, articles [3], [4], [5], [6], [7]) but most of them encounters serious technological limitation and/or has some other disadvantages which do not permit implementation of these methods in the near future. On the other hand, the SQL itself is not an absolute limit but, in particular, it depends on the dynamic properties of the test object which is used in the experiment. The well known example is the harmonic oscillator. Its response to a resonant force is relatively strong and it allows to use less sensitive meter (with larger measurement noise and therefore with smaller back action noise). Due to this property the harmonic oscillator allows to obtain sensitivity better than the SQL for the free mass when the signal frequency is close to the eigen frequency of the oscillator Ω_m [8], [9], [10], [11].

In the articles [8], [10] it was shown that it is possible to create very low noise mechanical rigidity using Fabry-Perot resonators with detuned pumping. In the article [11] it was also shown that such a rigidity exists in the signal-recycled topology of the gravitational-wave antennae and it permits to overcome the SQL for a free mass in narrow band.

One can imagine the following frequency dependent rigidity:

$$K(\Omega) = m\Omega^2 \qquad (40)$$

where m is the mass it is attached to, and Ω is an *arbitrary* observation frequency. In principle, such a rigidity would allow to obtain arbitrarily high sensitivity throughout the spectral range where the formula (40) is valid. On the other hand, it is well known that the mechanical rigidity created by parametrical opto-mechanical systems can be frequency dependent. In this article we show that the mechanical rigidity frequency dependence in large-scale interferometric meters with bandwidth comparable to or smaller than the signal frequency can be close to the formula (40) in some spectral band.

The simple example: Second-order-pole regime

Consider the simplified interferometric detector scheme presented in Fig. 4. Here the signal force with the amplitude F_{signal} which had to be detected, acts on the test mass m. This mass serves also as mirror M1 and together with second mirror M2 forms Fabry-Perot resonator. In this article we suppose that refraction of the mirror M1 is equal to unity and there is no absorption in the mirror M2.

The resonator is pumped at the frequency ω_{pump} which is detuned far from its eigen frequency ω_o:

$$\delta = \omega_{pump} - \omega_o \gg \gamma \,, \tag{41}$$

where γ is the half-bandwidth of the resonator. This detuned pumping creates a ponderomotive rigidity. One of the reflected beam quadrature amplitudes is measured, giving information about the mirrors relative position.

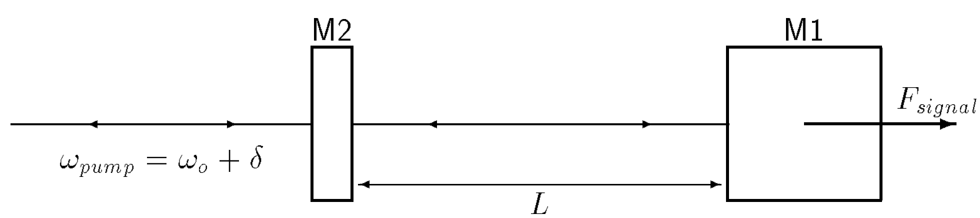

FIG. 4. Simplified scheme of the interferometric detector

We will refer to this simple scheme in this article but it can be shown that all results obtained here are valid for the signal-recycled topology [12] planned for the second stage of the LIGO program.

By solving this system equations of motion it is easy to show that if $\gamma \to 0$ then mechanical rigidity created by the optical pumping will be equal to

$$K(\Omega) \approx \frac{2\omega_o \mathcal{E} \delta}{L^2(\delta^2 - \Omega^2)} \tag{42}$$

where Ω is the observation frequency, $\mathcal{E}$ is the optical energy stored in the resonator, and L is the resonator length.

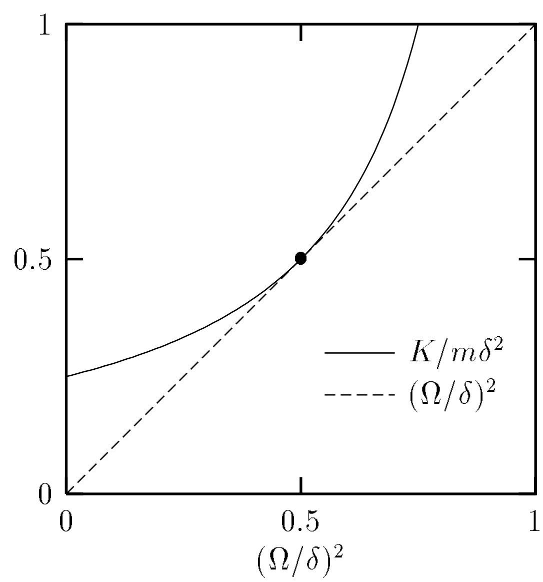

FIG. 5. Second-order pole ($\gamma \to 0$)

Our goal is to set $K(\Omega)$ as close to the ideal frequency dependence (40) as possible nearby some given value of Ω, so we require that

$$K(\Omega) = m\Omega^2 \tag{43}$$

and

$$\frac{dK(\Omega)}{d\Omega} = \frac{d(m\Omega^2)}{d\Omega}\,. \tag{44}$$

It is easy to show that these conditions can be fulfilled if (and only if)

$$\Omega = \Omega_2 \equiv \frac{\delta}{\sqrt{2}} \tag{45}$$

and

$$\mathcal{E} = \frac{mL^2\delta^3}{8\omega_o} = \frac{mL^2\Omega_2^3}{2\sqrt{2}\omega_o}\,. \tag{46}$$

In this case susceptibility of test object which consists of mass m and such a rigidity

$$\chi(\Omega) = \frac{1}{-m\Omega^2 + K(\Omega)} \tag{47}$$

will have a second-order pole at the frequency Ω_2, *i.e* if $|\Omega - \Omega_2| \ll \Omega$ then we will obtain

$$-m\Omega^2 + K(\Omega) \approx 4m(\Omega - \Omega_2)^2 \tag{48}$$

where subscript "2" means "second-order pole" (see Fig. 5, where second-order-pole point marked by "•"). It means if the signal force has the form of a sinusoidal train with duration τ_F and the mean frequency $\Omega_F \simeq \Omega_2$ then the amplitude of the mass m oscillations caused by this force will be proportional to[1]

$$x_{signal} \sim \frac{F_{signal}\tau_F^2}{m} \tag{49}$$

[1]We want to remind that the free mass has second-order pole at zero frequency, and the harmonic oscillator has first-order pole at resonance frequency.

(in this section we omit all numerical factors of the order of unity). On the other hand, it can be shown that the Standard Quantum Limit for such a second-order-pole system is equal to

$$x_{SQL}^{(2)} \sim \sqrt{\frac{\hbar \tau_F}{m}}\,. \tag{50}$$

Hence using this system and ordinary position meter, it is possible to detect the force

$$F_{signal} \sim \frac{m x_{SQL}^{(2)}}{\tau_F^2} = F_{SQL}^{(2)} = \sqrt{\frac{\hbar m}{\tau_F^3}}\,. \tag{51}$$

This value is $\Omega_F \tau_F$ times smaller than the SQL value corresponding to the free test mass

$$F_{SQL}^{free\ mass} = \sqrt{\frac{\hbar m \Omega_F^2}{\tau_F}} \tag{52}$$

and $\sqrt{\Omega_F \tau_F}$ times smaller than the SQL for the harmonic oscillator with ordinary frequency-independent rigidity,

$$F_{SQL}^{oscillator} = \frac{\sqrt{\hbar m \Omega_F}}{\tau_F}\,. \tag{53}$$

It had to be noted that the energy (46) is close to the energy

$$\mathcal{E} = \frac{m L^2 \Omega^3}{2\omega_o}\,. \tag{54}$$

which is necessary to achieve the SQL using traditional scheme of the interferometric position meter.

Sensitivity for different regimes of the frequency-dependent rigidity

In this section we will use spectral approach based on the total net noise of the meter (see article [13]). This noise is normalized in such a way that the signal-to-noise ratio is equal to

$$\frac{s}{n}=\int_{-\infty}^{\infty}\frac{|F_{signal}(\Omega)|^2}{S_{total}(\Omega)}\,\frac{d\Omega}{2\pi}\,, \tag{55}$$

where $F_{signal}(\Omega)$ is the spectrum of the signal force, and $S_{total}(\Omega)$ is the spectral density of this noise.

In the case of the interferometric detector (see Fig. 4) spectral density of the net noise is equal to

$$S_{total}(\Omega)=S_F^{eff}(\Omega)+\chi_{eff}^{-2}(\Omega)S_x(\Omega)\,, \tag{56}$$

where

$$S_F^{eff}(\Omega)=\frac{\hbar^2}{4S_x(\Omega)} \tag{57}$$

is the residual back-action noise of the meter (*i.e.* part of the back-action noise S_F which does not correlate with the measurement noise),

$$S_x(\Omega)=\frac{\hbar L^2}{8\omega_o\mathcal{E}\gamma}\times\frac{\Omega^4+2\Omega^2(\gamma^2-\delta^2)+(\gamma^2+\delta^2)^2}{\Omega^2+\gamma^2} \tag{58}$$

is the measurement noise,

$$\chi_{eff}(\Omega)=\frac{1}{-m\Omega^2+K_{eff}(\Omega)} \tag{59}$$

is the effective susceptibility of the system, and

$$K_{eff}=\frac{2\omega_o\mathcal{E}\delta}{L^2}\times\frac{3\gamma^2+\delta^2-\Omega^2}{\Omega^4+2\Omega^2(\gamma^2-\delta^2)+(\gamma^2+\delta^2)^2} \tag{60}$$

is the effective rigidity which is the sum of two terms: (i) the real physical rigidity which exists in the system due to the dependence of the optical energy in the resonator on the mirrors position, and (ii) the "virtual" rigidity introduced by the cross-correlation of the measurement noise and back-action noise (see article [14]). It should be noted that in our case the real rigidity is much larger than the "virtual" one. However, it is the "virtual" rigidity that compensates the imaginary part of the real physical rigidity which describes dynamical instability of the system. In other words, the instability does exist and must be compensated by some feed-back scheme but the meter does not "see" it.

Expressions (58,60) are obtained for the case where the phase quadrature amplitude of the output optical wave is measured. Our results does not depend essentially on which quadrature amplitude is measured but choosing of the phase quadrature amplitude provides slightly better results and also allows to simplify the formulae.

The behavior of the $K_{eff}(\Omega)$ is rather sophisticated and allows a several different regimes, depending on the pumping energy, resonator bandwidth and detuning: with three first-order poles [Fig. c(a)]; with one second-order and one first-order poles [Fig. c(b,c)]; and with one third-order pole [Fig. c(d)]. Which one should be chosen depends on the signal form. Detailed analysis of all of them exceeds the frames of this short article. One of these regimes was considered in details in the article [11]. Here we consider two other regimes which for our opinion are the most interesting ones from both theoretical and "consumer" points of view.

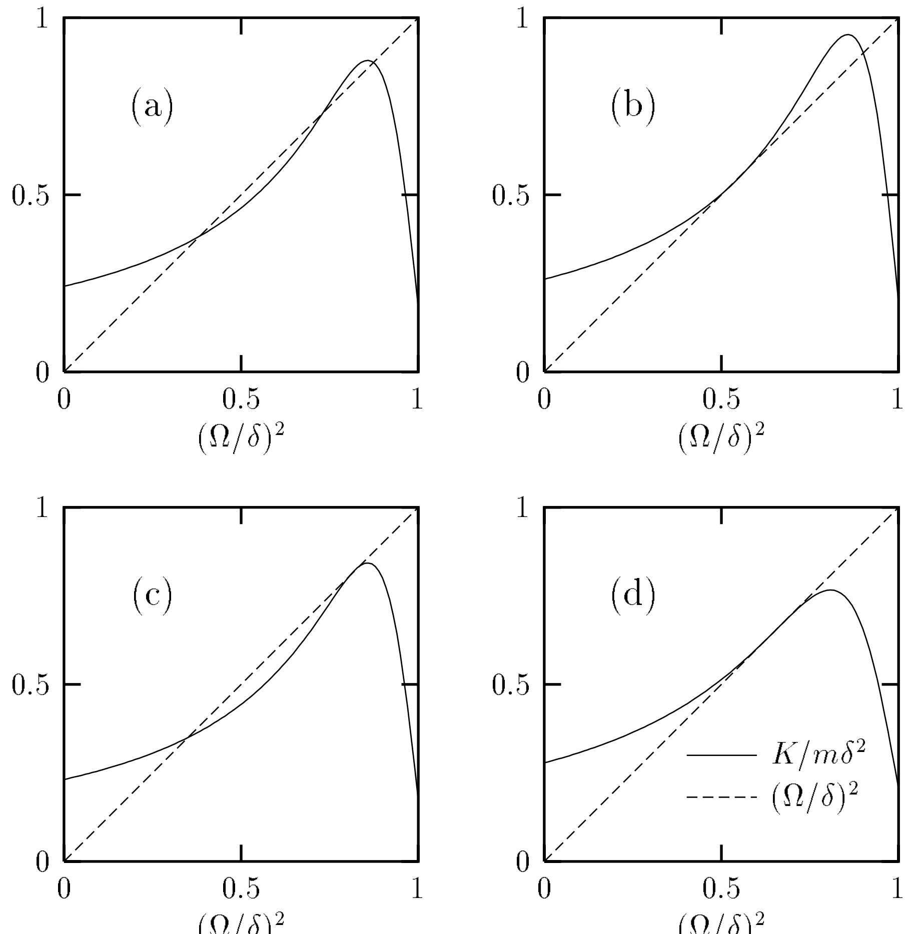

FIG. 6. Different regimes of the frequency-dependent rigidity: (a) — three first-order poles; (b,c) — one second-order and one first-order poles; (d) — one third-order pole

The second-order-pole regime If the bandwidth of the Fabry-Perot resonator is small, $\gamma \ll \delta$, and the pumping energy is equal to[2]

$$\mathcal{E} \approx \frac{mL^2\delta^3}{8\omega_o}\left(1 + \frac{6\gamma^2}{\delta^2}\right) , \tag{61}$$

then in the narrow vicinity of the frequency

---

[2]The exact expressions are too cumbersome so we present here only second-order Taylor expansions with respect to small parameter γ/δ

$$\Omega_2 \approx \sqrt{\frac{\delta^2 + 11\gamma^2}{2}} \tag{62}$$

the formula (56) can be presented as

$$S_{total}(\Omega) = \hbar m \delta^2 \left[\frac{\gamma}{2\delta} + \frac{2\delta}{\gamma}\,\frac{(\Omega - \Omega_2)^4}{\Omega_2^4}\right]. \tag{63}$$

The value of γ/δ can be adjusted to provide minimum of this spectral density at the edges of some given spectral band $\Omega_2 \pm \Delta\Omega/2$:

$$\frac{\gamma}{\delta} = \frac{1}{2}\left(\frac{\Delta\Omega}{\Omega_2}\right)^2. \tag{64}$$

In this case there will be

$$S_{total}(\Omega_2 \pm \Delta\Omega/2) = \hbar m (\Delta\Omega)^2. \tag{65}$$

This is the spectral equivalent of the formula (51).

In Fig. 7 spectral density of the total noise (56) is presented for several values of γ and for the pumping energy (61) corresponding to the second-order pole (dashed line is the SQL level).

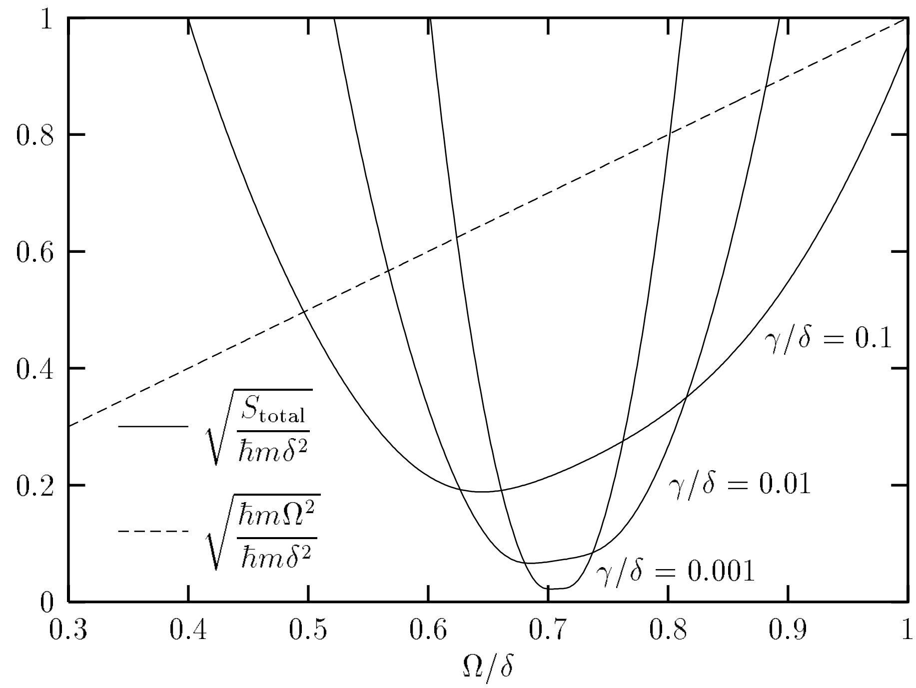

FIG. 7. Sensitivity for the second-order-pole regime

It is useful to compare sensitivity of this regime with the sensitivity provided by the usual probe oscillator with frequency independent rigidity and with eigen frequency Ω_m. In the latter case (see article [10])

$$\xi^2 \equiv \frac{S_{total}(\Omega_m \pm \Delta\Omega/2)}{S_{SQL}(\Omega_m)} = \frac{\Delta\Omega}{\Omega_m}\,, \tag{66}$$

where $S_{SQL}(\Omega) = \hbar m\Omega^2$ is the spectral density corresponding to the SQL for the free test mass. In the case of second-order pole regime will be

$$\xi^2 \equiv \frac{S_{total}(\Omega_2 \pm \Delta\Omega/2)}{S_{SQL}(\Omega_2)} = \left(\frac{\Delta\Omega}{\Omega_2}\right)^2 = \frac{2\gamma}{\delta}\,. \tag{67}$$

The third-order-pole regime Parameters of the scheme can be tuned also to create the third order pole of the effective susceptibility (59) by setting

$$\mathcal{E} = \frac{9\sqrt{177} - 113}{49} \times \frac{mL^2\delta^3}{\omega_o} \approx \frac{0.14 mL^2\delta^3}{\omega_o} \tag{68}$$

and

$$\frac{\gamma}{\delta} = \frac{\sqrt{280 - 21\sqrt{177}}}{7} \approx 0.11\,. \tag{69}$$

The pole frequency is equal to

$$\Omega_3 = \sqrt{\frac{2\sqrt{177} - 22}{7}}\,\delta \approx 0.81\delta\,. \tag{70}$$

In Fig. 8 spectral density of the total noise (56) is presented for the case of the third-order-pole regime.

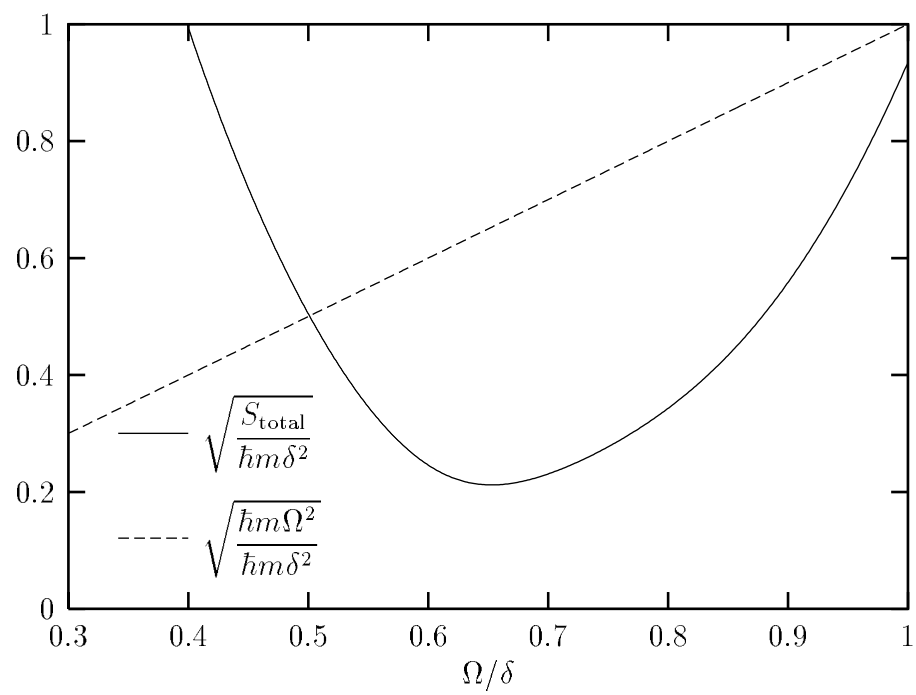

FIG. 8. Sensitivity for the third-order-pole regime

It is necessary to note that this third-order-pole regime is "overpumped": the second term in the formula (56), that is proportional to the measurement noise, is several orders of magnitude smaller than the first one (back-action noise) in the frequency area of interest. It is evident from Fig. 9, where these two terms are plotted separately. Usually, in such a situation the reduction of the total noise is possible by increasing the measurement noise and proportional decreasing the back-action noise due to using, for example, smaller value of the pumping energy. Unfortunately, within the framework of our simple scheme it is impossible because the same optical pumping is used both for measurement and for creating the rigidity. There is no additional "degree of freedom" here: values of all parameters are fixed by the equations (68,69). It is probable, however, that more sophisticated topologies based on use of separate optical modes for measurement and for creating rigidity, or/and which eliminate back-action noise by using variational measurement [5,6,15], will allow to create "well-balanced" third-order-pole regime with very low total noise.

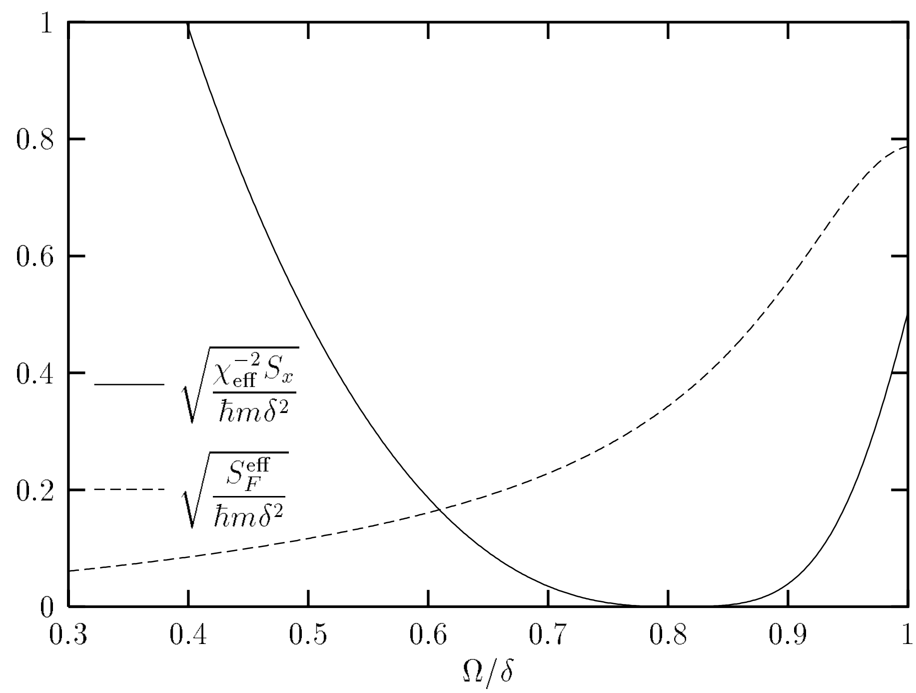

FIG. 9. Measurement noise and back-action noise for the third-order-pole regime

Conclusion

It is evidently impossible to consider thoroughly in one short article all the possible variants of the use of the frequency-dependent rigidity which exists in large-scale optical resonators. Such a consideration has to be based on *a priori* information about the signal spectrum provided, for example, by astrophysical predictions in the similar as it had been done in the article [11]. It is evident, however, that:

- The second-order-pole regime allows to "dive" deep below the SQL in the narrow spectral band $\Delta\Omega$ which is, however, much wider than if the usual frequency independent rigidity is used [compare formulae (66) and (67)]. The recent achievements in fabrication of high-reflectivity mirrors [16] allows to expect that it will be possible to obtain relaxation time of the large-scale interferometers $\gamma^{-1} \gtrsim 1\,\mathrm{s}$ and thus to reach the sensitivity at the level of $\xi^2 \lesssim 10^{-3}$, if $\Omega \sim \delta \sim 10^3\,\mathrm{s}^{-1}$. It is important that the pumping energy in this regime does not depend on the sensitivity and remains approximately equal to the energy (54) which is necessary to achieve the SQL in the traditional scheme of the interferometric position meter.

- The third-order-pole regime provides sensitivity a few times better than the Standard Quantum Limit in relatively wide spectral band and at extremely low level of the measurement noise in this band. This regime looks as a good candidate for use in advanced topologies of the gravitational-wave antennae.

REFERENCES

[1] V.B.Braginsky, Sov. Phys. JETP **26**, 831 (1968).

[2] K.S.Thorne, *Three Hundred Years of Gravitation*, Cambridge University Press, 1987.

[3] V.B.Braginsky, M.L.Gorodetsky, F.Ya.Khalili, Physics Letters A **232**, 340 (1997).

[4] V.B.Braginsky, M.L.Gorodetsky, F.Ya.Khalili, Physics Letters A **246**, 485 (1998).

[5] A.B.Matsko, S.P.Vyatchanin, JETP **77**, 218 (1993).

[6] S.P.Vyatchanin, Physics Letters A **239**, 201 (1998).

[7] H.J.Kimble, Yu.Levin, A.B.Matsko, K.S.Thorne and S.P.Vyatchanin, Physical Review D , in press (2001).

[8] V.B.Braginsky, F.Ya.Khalili, Physics Letters A **257**, 241 (1999).

[9] F.Ya.Khalili, Optics and Spectroscopy **91**, 550 (2001).

[10] V.B.Braginsky, F.Ya.Khalili, S.P.Volikov, Physics Letters A A **287**, 31 (2001).

[11] A.Buonanno, Y.Chen, Physical Review D , in press (2001).

[12] B.Meers, Physical Review D **38**, 2217 (1988).

[13] V.B.Braginsky, M.L.Gorodetsky, F.Ya.Khalili and K.S.Thorne, Physical Review D **61**, 044002 (2000).

[14] A.V.Syrtsev, F.Ya.Khalili, JETP **79**, 409 (1994).

[15] S.L.Danilishin, F.Ya.Khalili, S.P.Vyatchanin, Physics Letters A **278**, 123 (2000).

[16] G.Rempe, R.Tompson, H.J.Kimble, Optics Letters **17**, 363 (1992).

Appendix G. Parametric Oscillatory Instability in Fabry-Perot (FP) Interferometer

Introduction

The full scale terrestrial gravitational wave antennae are in process of assembling and tuning at present. One of these antennae (LIGO-I project) sensitivity expressed in terms of the metric perturbation amplitude is projected to achieve soon the level of $h \simeq 1 \times 10^{-21}$ [1,2]. In 2008 the projected level of sensitivity has to be not less than $h \simeq 1 \times 10^{-22}$ [3]. This value is scheduled to achieve by substantial improvement of the test masses (mirrors in the big FP resonator) isolation from different sources of noises and by increasing the optical readout system sensitivity. This increase is expected to be obtained by rising the value of optical energy $\mathcal{E}_0$ stored in the FP resonator optical mode: $\mathcal{E}_0 > 30$ J (it corresponds to the circulating power W bigger than 1 megaWatt). So high values of $\mathcal{E}_0$ and W may be a source of the nonlinear effects which will prevent from reaching the projected sensitivity of $h \sim 1 \times 10^{-22}$. Authors of this article already described two such effects: photo-thermal shot noise [4] (the random absorption of optical photons in the surface layer of the mirror causes the fluctuating of mirror surface due to nonzero coefficient of thermal expansion) and photo-refractive shot noise [5] (the same random absorption of optical photons causes the fluctuations of the reflected wave phase due to the dependence of refraction index on temperature). In this paper we analyze undesirable effect of parametric instability — another "trap" of pure dynamical nonlinear origin which (being ignored) may cause very substantial decrease of the antennae sensitivity and even may make the antenna unable to work properly.

It is appropriate to remind that nonlinear coupling of elastic and light waves in continuous media produces Mandelstam-Brillouin scattering. It is a classical parametric effect, however, it is often explained in terms of quantum physics: one quantum $\hbar\omega_0$ of main optical wave transforms into two, *i. e.* $\hbar\omega_1$ in the additional optical wave (Stokes wave: $\omega_1 < \omega_0$) and $\hbar\omega_m$ in the elastic wave so that $\omega_0 = \omega_1 + \omega_m$ (it is Manley-Rowe condition for parametric process). The irradiation into the anti-Stokes wave is also possible ($\omega_1 = \omega_0 + \omega_m$), however, in this case the part of energy is taken from the elastic wave. The physical "mechanism" of this coupling is the dependence of refractive index on density which is modulated by elastic waves. If the main wave power is large enough the stimulated scattering will take place, the amplitudes of elastic and Stokes waves will increase substantially. The physical description is the following: the flux of energy into these waves is so large that before being irradiated from the volume of interaction, the oscillations with frequencies ω_1 and ω_m stimulate each other substantially increasing the power taken from the main wave. Note that stimulated scattering causes irradiation only into Stokes wave because the additional energy pump into elastic wave must take place for radiation into anti-Stokes wave.

In gravitational wave antennae elastic oscillations in FP resonator mirrors will interact with optical ones being coupled parametrically due to the boundary conditions on one hand, and due to the ponderomotive force on the other hand. Two optical modes may play roles of the main and Stokes waves. High quality factors of these modes and of the elastic one will increase the effectiveness of the interaction between them and may give birth to the parametric oscillatory instability which is similar to stimulated Mandelstam-Brillouin effect [6]. This instability may create a specific upper limit for the value of energy $\mathcal{E}_0$.

It is worth to note that this effect of parametric instability is a particular case of the more general phenomenon related to the dynamical back action of parametric displacement meter on mechanical oscillator or free mass. This dynamical back action was analyzed and observed more than 30 years ago [7,8]. Usually parametric meter consists of e.m. resonator with high quality factor Q (radiofrequency, microwave or optical ones) and high frequency stability pumping self-sustained oscillator. The displacement of the resonator movable element modulates its eigenfrequency which in its turn produces the modulation of the e.m. oscillations amplitude (it can produce also phase or output power modulations). If the experimentalist attaches a probe mass to the movable element of the meter he is inevitably confronted with the effect of dynamical back action, the ponderomotive force produces a rigidity and due to finite e.m. relaxation time — a mechanical friction. Both these values may be positive and negative ones. In the case when the negative friction is sufficiently high the behavior of mechanical oscillator and meter becomes oscillatory unstable. This effect was observed and explained for the case when value of mechanical frequency ω_m was substantially smaller than the bandwidth of e.m. resonator [7,8]. In this article we analyze the parametric oscillatory instability in two optical modes of FP resonator and elastic mode of the mirror. In this case the value of ω_m is much larger than the bandwidth of the optical modes.

In section II we present the analysis of this effect for simplified one-dimensional model which permits to obtain approximate estimates for the instability conditions. In section III we present considerations and preliminary estimates for nonsimplified three-dimensional model, and in section c — the program of necessary mode numerical analysis.

Simplified one-dimensional model

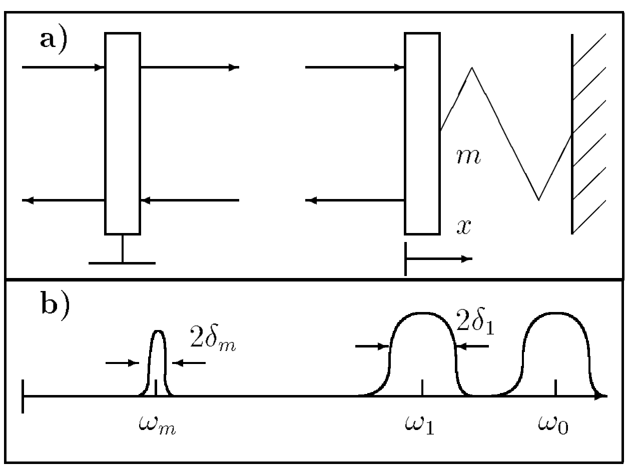

FIG. 10. Scheme of FP resonator with movable mirror (a) and frequency diagram (b).

For approximate estimates we present in this section the simplified model analysis where we assume that:

- The mechanical oscillator (model of mirror) is a lumped one with single mechanical degree of freedom (eigenfrequency ω_m and quality factor $Q_m = \omega_m/2\delta_m$).

- This oscillator mass m is the FP resonator right mirror (see fig. 10) having ideal reflectivity and the value of m is of the order of the total mirror's mass.

- The left mirror (through which FP resonator is pumped) has an infinite mass, no optical losses and finite transmittance $T = 2\pi L/(\lambda_0 Q_{opt})$ (λ_0 is the optical wavelength, Q_{opt} is the quality factor, L is the distance between the mirrors).

- We take into account only the main mode with frequency ω_0 and relaxation rate $\delta_0 = \omega_0/2Q_0$ and Stokes mode with ω_1 and $\delta_1 = \omega_0/2Q_1$ correspondingly (Q_0 and Q_1 are the quality factors), $\omega_0 - \omega_1 \simeq \omega_m$.

- Laser is pumping only the main mode which stored energy $\mathcal{E}_0$ is assumed to be a constant one (approximation of constant field).

It is possible to calculate at what level of energy $\mathcal{E}_0$ the Stokes mode and mechanical oscillator becomes unstable. The origin of this instability can be described qualitatively in the following way: small mechanical oscillations with the resonance frequency ω_m modulate the distance L that causes the exitation of optical fields with frequencies $\omega_0 \pm \omega_m$. Therefore, the Stokes mode amplitude will rise linearly in time if time interval is shorter than δ_1^{-1}. The presence of two optical fields with frequencies ω_0 and ω_1 will produce the component of ponderomotive force (which is proportional to square of sum field) on difference frequency $\omega_0 - \omega_1$. Thus this force will increase the initially small amplitude of mechanical oscillations. In other words, we have to use two equations for Stokes mode and mechanical oscillator and find the conditions when this "feedback" prevails the damping which exists due to the finite values of Q_m and Q_1. Below we present only the scheme of calculations (see details in Appendix c).

We write down the field components of optical modes and the displacement x of mechanical oscillator in rotating wave approximation:

$$E_0 = A_0[D_0 e^{-i\omega_0 t} + D_0^* e^{i\omega_0 t}],$$

$$E_1 = A_1[D_1 e^{-i\omega_1 t} + D_1^* e^{i\omega_1 t}],$$

$$x = X e^{-i\omega_m t} + X^* e^{i\omega_m t},$$

where D_0 and D_1 are the slowly changing complex amplitudes of the main and Stokes modes correspondingly and X is the slowly changing complex amplitude of mechanical displacement. Normalizing constants $A_0,\ A_1$ are chosen so that energies $\mathcal{E}_{0,1}$ stored in each mode are equal to $\mathcal{E}_{0,1} = \omega_{0,1}^2 |D_{0,1}|^2/2$. Then it is easy to obtain the equations for slowly changing amplitudes:

$$\partial_t D_1 + \delta_1 D_1 = \frac{iX^*\, D_0\omega_0}{L}\, e^{-i\Delta\omega t}, \tag{71}$$

$$\partial_t X + \delta_m X = \frac{i\, D_0 D_1^* \omega_0\omega_1}{m\omega_m L}\ e^{-i\Delta\omega t}, \tag{72}$$

where $\Delta\omega = \omega_0 - \omega_1 - \omega_m$ is the possible detuning. Remind that we assume D_0 as a constant.

One can find the solutions of (71, 72) in the following form $D_1(t) = D_1 e^{(\lambda - \Delta\omega/2)t}$, $X^*(t) = X^* e^{(\lambda + \Delta\omega/2)t}$ and write down the characteristic equation. The parametric oscillatory instability will appear if real part of one of the characteristic equation roots is positive.

In LIGO design the values of δ_0 and δ_1 are of the order of the bandwidth the gravitational burst spectrum is expected to lie in, i.e. $\simeq 2\pi \times 100$ s^{-1}. On the other hand many efforts were made to reduce the value of δ_m to the lowest possible level and thus to decrease the threshold of sensitivity caused by Brownian noise. In existing today fused silica mirrors $Q_m \simeq 10^6 - 2\times 10^7$ and even for $\omega_m = 10^7$ s^{-1} the value of $\delta_m \leq 10$ s^{-1}. Thus we can assume that $\delta_m \ll \delta_1$ and obtain the instability condition in simple form:

$$\frac{\mathcal{R}_0}{\left(1 + \frac{\Delta\omega^2}{\delta_1^2}\right)} > 1, \tag{73}$$

$$\mathcal{R}_0 = \frac{\mathcal{E}_0}{2mL^2\omega_m^2}\,\frac{\omega_1\omega_m}{\delta_1\delta_m} = \frac{2\mathcal{E}_0 Q_1 Q_m}{mL^2\omega_m^2}\,. \tag{74}$$

For estimates we assume parameters corresponding to LIGO-II to be:

$$\begin{aligned}
\omega_m &= 2\times 10^5 \text{ sec}^{-1}, \ \delta_m = 5\times 10^{-3} \text{ sec}^{-1}, \\
\delta_1 &= 6\times 10^2 \text{ sec}^{-1}, \ \omega_1 \simeq 2\times 10^{15} \text{ sec}^{-1}, \\
\mathcal{E}_0 &\simeq 3\times 10^8 \text{ erg}, \quad L = 4\times 10^5 \text{ cm} \\
m &= 10^4 \text{ g},
\end{aligned} \tag{75}$$

The mechanical frequency ω_m is about the frequency of the lowest mirror elastic (longitudinal or drum) mode and it has the same order as the intermodal interval $\sim \pi c/L \simeq 2\times 10^5$ sec^{-1} between optical modes of FP resonator. The mechanical relaxation rate δ_m corresponds to the loss angle $\phi \simeq 5\times 10^{-8}$ (quality factor $Q_m \simeq 2\times 10^7$) for fused silica. The value of energy $\mathcal{E}_0$ corresponds to the value of circulating power about $W \simeq c\mathcal{E}_0/2L \simeq 10^{13}$ erg/s $= 10^6$ Watt.

For these parameters we have obtained the estimate of coefficient $\mathcal{R}_0$ for the resonance case ($|\Delta\omega| \ll \delta_1$):

$$\mathcal{R}_0 \simeq 300 \gg 1$$

It means that the critical value of stored energy $\mathcal{E}_0$ for the instability initiation will be 300 times smaller than the planned value $\simeq 3\times 10^8$ erg $= 30$ J [3].

For nonresonance case and planned value of $\mathcal{E}_0$ the "borders" of detuning $\Delta\omega_{crit}$ within the system is unstable, are relatively large: $\Delta\omega_{crit} = \delta_1\sqrt{R_0} \simeq 1.7\times 10^4$ sec^{-1}.

Considerations of Three-Dimensional Modes Analysis

The numerical estimates for the values of factor $\mathcal{R}_0$ and detuning $\Delta\omega$ obtained in the preceding section have to be regarded as some kind of warning about the reality of the

[3] It is worth to note that if sapphire is chosen then due to the larger value of Q_m the factor $\mathcal{R}_0$ will be even bigger: $\mathcal{R}_0 \simeq 5\times 10^3$. It is another argument which is not in favor of this material for mirrors.

undesirable parametric instability effect. In the simplified analysis we have ignored the nonuniform distribution of optical fields and of mechanical displacements over the mirror's surface. It is evident that more accurate analysis has to be done. Below we present several considerations about further necessary analysis.

The frequency range of "dangerous" optical and elastic modes

The values of the mirror's radius R and thickness H for LIGO-II are not yet finally defined. Due to the necessity to decrease the level of thermoelastic and thermorefractive noises [4,5,9,10] the size of the light spot on the mirror's surface is likely to be substantially larger than in LIGO-I and the light density distribution in the spot is not likely to be a gaussian one (to evade substantial diffractional losses) [10]. Thus the presented below estimates for gaussian optical modes may be regarded only as the first approximation in which the use of analytical calculations is still possible.

The resonance conditions $|\omega_0 - \omega_1 - \omega_m| < \delta_1$ may be obtained with a relatively high probability for many optical Stokes and mirror elastic modes combinations. If we assume the main optical mode to be gaussian one with waist radius w_0 of the caustic (the optical field amplitude distribution in the middle between the mirrors is $\sim e^{-r^2/w_0^2}$)), and if we assume also that the Stokes mode may be described by generalized Laguerre functions (Gauss-Laguerre beams) then the set of frequency distances $\Delta\omega_{\rm opt}$ between the main and Stokes modes is determined by three integer numbers:

$$\Delta\omega_{\rm optic} \simeq \frac{\pi c}{L}\left(K + \frac{2(2N+M)}{\pi}\arctan\frac{L\lambda_0}{2\pi w_0^2}\right), \tag{76}$$

where λ_0 is the wave length, $K = 0 \pm 1, \pm 2\ldots$ is the longitudinal index, $N = 0, 1, 2\ldots$, and $M = 0, 1, 2\ldots$ are the radial and angular indices.

For $w_0 \simeq 5.9$ cm the beam radius on the mirror's surface is equal to $w \simeq 6$ cm, corresponding to the level of diffractional losses about 20 ppm for mirror radius of $R = 14$ cm. In this case the equation (76) has the following form:

$$\Delta\omega_{\rm optic} \simeq (2.4\,K + 0.56\,N + 0.28\,M) \times 10^5\,{\rm s}^{-1}. \tag{77}$$

We see that the distance between optical modes is not so large, i.e. $\simeq 3\times10^4\,\mathrm{s}^{-1}$. In units of optical modes bandwidth $2\delta_1 \simeq 10^3\,\mathrm{s}^{-1}$ it is about $3\times10^4/2\delta_1 \simeq 30$. Thus assuming that the value of elastic mode frequency can be an arbitrary one we can roughly estimate the probability that the resonance condition is fulfilled as $\sim 1/30$.

The order of the distance $\Delta\omega_{m0}$ between the frequencies for the first several elastic modes is about $\Delta\omega_{m0} \simeq \pi v_s/d \simeq 2\times10^5\ \mathrm{s}^{-1}$ (d is the dimension of the mirror and v_s is the sound velocity). It is about one order larger than the distance between the optical modes. However, for higher frequencies ω_m these intervals become smaller and can be estimated by formula

$$\Delta\omega_m \simeq \frac{\pi\Delta\omega_{m0}^3}{2\omega_m^2}$$

Even for $\omega_m \simeq 6\times10^5\ \mathrm{s}^{-1}$ the intervals between the elastic and optical modes become equal to each other and has value about $\simeq 3\times10^4\,\mathrm{s}^{-1}$. And for $\omega_m \sim 10^7\ \mathrm{s}^{-1}$ the distances between elastic modes become of the order of optical bandwidth $2\delta_1$. Therefore, the resonance condition for these frequencies is practically always fulfilled.

On the other hand according to (74) the factor $\mathcal{R}_0$ decreases for higher elastic frequencies ω_m. In addition the loss angle in fused silica usually slightly increases for higher frequencies [11,12]. Assuming that the upper value $\omega_m \simeq 2\times10^6\ \mathrm{s}^{-1}$, $Q_m \simeq 3\times10^6$ and other parameters correspond to (75) we obtain $\mathcal{R}_0 \simeq 1$. Therefore, the elastic modes which "deserve" accurate calculations lie within the range between several tens and several hundreds kiloHerz. The total number of these modes is about several hundreds.

The Matching between the Mechanical Displacements and Light Density Distributions

The simplified model described in section c is approximately valid for the uniform over all the mirror's surface distribution of optical field density and pure longitudinal elastic mode. The equations for this model can be extended for any distributions of mechanical displacements in the chosen elastic mode and for any distribution of the light field density in chosen optical modes. This extension can be done by adding a dimensionless factor Λ in (73):

$$\frac{\mathcal{R}_0 \Lambda}{\left(1 + \frac{\delta\omega^2}{\delta_1^2}\right)} > 1, \tag{78}$$

$$\Lambda = \frac{V\left(\int f_0(\vec{r}_\perp)\, f_1(\vec{r}_\perp)\, u_z\, d\vec{r}_\perp\right)^2}{\int |f_0|^2 d\vec{r}_\perp \; \int |f_1|^2 d\vec{r}_\perp \; \int |\vec{u}|^2 dV}. \tag{79}$$

Here f_0 and f_1 are the functions of the distributions over the mirror's surface of the optical fields in the main and Stokes optical modes correspondingly, vector $\vec{u}$ is the spatial vector of displacements in elastic mode, u_z is the component of $\vec{u}$, normal to the mirror's surface, $\int d\vec{r}_\perp$ corresponds to the integration over the mirror's surface and $\int dV$ — over the mirror's volume V.

It is necessary to know the functions f_0, f_1, $\vec{u}$ in order to calculate the factors Λ for different mode combinations. But to the best of our knowledge there is no analytical form for $\vec{u}$ in the case of cylinder with free boundary conditions [11]. Our approximate estimates show that there is substantial number of modes combinations for which factor Λ is large enough to satisfy the condition (78) for parameters (75). We do not present the details of these estimates here because they are rather rough. It is evident that a complete numerical analysis which includes nongaussian distributions of optical fields is necessary to do.

Conclusion

The simplified model analysis of parametric oscillatory instability and considerations about the real model presented above may be regarded only as the first step along the route to obtain a guarantee to evade this nondesirable effect. Summing up we may formulate several recommendations for the next steps:

1. Due to the finite size of the mirror and to the use of the nongaussian distribution of light density we think that the accurate numerical analysis of different optical and elastic mode combinations (candidates for the parametric instability) is inevitably necessary. This problem (numerical calculations for the elastic modes) has been already solved partialy [13].

2. In the same time the numerical analysis may not give an absolute guarantee because the fused silica pins and fibers will be attached to the mirror. This attachment will change the elastic modes frequency values (and may be also the distribution). In addition the unknown Young modulus and fused silica density inhomogeneity will limit the numerical analysis accuracy. Thus the direct measurements for several hundreds of probe mass elastic modes eigenfrequencies values and quality factors are also necessary.

3. When more "dangerous" candidates of elastic and Stokes modes will be known, their undesirable influence can be depressed. For example it can be done by small the change of mirror's shape.

4. It is also reasonable to perform direct tests of the optical field behavior with smooth increase of the input optical power: it will be possible to register the appearence of the photons at the Stokes modes and the rise of the Q_m in the corresponding elastic mode until the power W in the main optical mode is below the critical value.

5. Apart from above presented case of the oscillatory instability it is likely that there are similar instability in which other mechanical modes are involved (especialy violin ones which also have eigen frequencies several tens kHz and higher). There are also additional instability for the pendelum mode in the mirror's suspension (in the case of small detuning of pumping optical frequency out of resonance). These potencial "dangers" also deserve accurate analysis.

We think that the parametric oscillatory instability effect can be excluded in the laser gravitational antennae after this detailed investigation.

Acknowledgements

Authors are very grateful to H. J. Kimble, S. Witcomb and especially to F. Ya. Khalili for help, stimulating discussions and advises. This work was supported in part by NSF and

Caltech grants and by Russian Ministry of Industry and Science and Russian Foundation of Basic Researches.

Appendix A: Lagrangian Approach

Let us denote $q_0(t)$ and $q_1(t)$ as generalized coordinates for the FP resonator optical modes with frequencies ω_0 and ω_1 correspondingly, so that their vector potentials $(A_0,\ A_1)$, electrical $(E_0,\ E_1)$ and magnetic $(H_0,\ H_1)$ fields are the following:

$$A_i(t) = \sqrt{\frac{2\pi\, c^2}{S_i L}} \left(f_i e^{ik_i z} - f_i^* e^{-ik_i z}\right)\, q_i(t),$$

$$E_i(t) = -\sqrt{\frac{2\pi}{S_i L}} \left(f_i e^{ik_i z} - f_i^* e^{-ik_i z}\right)\, \partial_t q_i(t),$$

$$H_i(t) = \sqrt{\frac{2\pi}{S_i L}} \left(f_i e^{ik_i z} + f_i^* e^{-ik_i z}\right)\, \omega_i q_i(t),$$

$$f_i = f_i(\vec r_\perp, z), \quad S_i = \int |f_i|^2 \vec d r_\perp.$$

Let also denote $x(t)$ as generalized coordinate of the considered elastic oscillations mode with displacement spatial distribution described by the vector $\vec u(\vec r)$. Now we can write down the lagrangian:

$$\mathcal{L} = \mathcal{L}_0 + \mathcal{L}_1 + \mathcal{L}_m + \mathcal{L}_{int},$$

$$\mathcal{L}_0 = \int \frac{L(\langle E_0\rangle^2 - \langle H_0\rangle^2)}{8\pi}\, \vec d r_\perp = \frac{\partial_t q_0^2}{2} - \frac{\omega_0^2 q_0^2}{2},$$

$$\mathcal{L}_1 = \frac{\partial_t q_1^2}{2} - \frac{\omega_0^2 q_1^2}{2},$$

$$\mathcal{L}_m = \frac{M(\partial_t x)^2}{2} - \frac{M\omega_m^2 x^2}{2},$$

$$M = \rho \int_V |\vec u(\vec r)|^2\, dV,$$

$$\mathcal{L}_{int} = -\int \left.\frac{x\, u_z \langle H_0 + H_1\rangle^2}{8\pi}\right|_{z=0} d\vec r_\perp =$$

$$= -2\omega_0\omega_1\, q_0 q_1\, B\, \frac{x}{L},$$

$$B = \frac{\int f_0(\vec r_\perp) f_1(\vec r_\perp) u_z d\vec r_\perp}{\sqrt{\int |f_0|^2 d\vec r_\perp \int |f_1|^2 d\vec r_\perp}}$$

We consider only one mechanical mode below. Now we can write down the equations of motion (adding losses in each degree of freedom):

$$\begin{aligned}
\partial_t^2 q_0 + 2\delta_0 \partial_t q_0 + \omega_0^2 q_0 &= -B\frac{2x}{L}\,\omega_0\omega_1 q_1,\\
\partial_t^2 q_1 + 2\delta_1 \partial_t q_1 + \omega_1^2 q_1 &= -B\,\frac{2x}{L}\,\omega_1\omega_0\, q_0,\\
\partial_t^2 x + 2\delta_m \partial_t x + \omega_m^2 x &= -B\frac{2\omega_0\omega_1}{ML}\, q_0\, q_1.
\end{aligned}$$

Introducing slowly varying amplitudes we can rewrite these equations as:

$$\begin{aligned}
q_0(t) &= D_0(t)\, e^{-i\omega_0 t} + D_0^*(t)\, e^{i\omega_0 t},\\
q_1(t) &= D_1(t)\, e^{-i\omega_1 t} + D_1^*(t)\, e^{i\omega_1 t},\\
x(t) &= X(t)\, e^{-i\omega_m t} + X^*(t)\, e^{i\omega_m t},\\
\Delta\omega &= \omega_0 - \omega_1 - \omega_m,
\end{aligned}$$

$$\partial_t D_0 + \delta_0 D_0 = \frac{iBX\, D_1\omega_1}{L}\, e^{i\Delta\omega t},$$

$$\partial_t D_1 + \delta_1 D_1 = \frac{iBX^*\, D_0\omega_0}{L}\, e^{-i\Delta\omega t}, \tag{80}$$

$$\partial_t X + \delta_m X = \frac{i\, BD_0 D_1^*\omega_0\omega_1}{M\omega_m L}\; e^{-i\Delta\omega t}, \tag{81}$$

We can see that this system (81, 80) coincides with (72, 71) if $B = 1$, and $M = m$.

For the simplest resonance case $\delta\omega = 0$ it is easy to substitute (81) into (80) and to obtain the condition of parametric instability (in the frequency domain):

$$D_1(\delta_1 - i\Omega) = \frac{iBD_0\omega_0}{L} \times \frac{-i\, BD_0^* D_1\omega_0\omega_1}{M\omega_m L(\delta_m + i\Omega)},$$

Condition of instability:

$$1 < \frac{B^2|D_0|^2\omega_0^2\omega_1}{M\omega_m L^2\delta_1\delta_m}$$

Now we can express the energy $\mathcal{E}_0$ in mode "0" in terms of $|D_0|^2$:

$$\begin{aligned}
\mathcal{E}_0 &= \frac{\partial_t q_0^2}{2} + \frac{\omega_0^2 q_0^2}{2} =\\
&= \frac{1}{2}\Big((-i\omega_0)^2\left[D_0\, e^{-i\omega_0 t} - D_0^*\, e^{i\omega_0 t}\right]^2 +\\
&\qquad + \omega_0^2\left[D_0\, e^{-i\omega_0 t} + D_0^*\, e^{i\omega_0 t}\right]^2\Big) =\\
&= 2\omega_0^2|D_0|^2.
\end{aligned}$$

Now we can write down the condition of parametric instability in the following form:

$$\frac{\mathcal{E}_0 B}{2m\omega_m^2 L^2} \times \frac{\omega_1\omega_m}{\delta_1\delta_m} > 1, \tag{82}$$

$$\Lambda = \frac{B^2 m}{M} = \frac{V\left(\int f_0(\vec{r}_\perp)f_1(\vec{r}_\perp)u_z d\vec{r}_\perp\right)^2}{\int |f_0|^2 d\vec{r}_\perp \int |f_1|^2 d\vec{r}_\perp \int |\vec{u}|^2 dV} \tag{83}$$

which accurately coincides with (78, 79).

Let us deduce the instability condition for nonresonance case. We are looking for the solution of (71, 72) in the following form:

$$D_1(t) = D_1 e^{\lambda_- t}, \quad X^*(t) = X^* e^{\lambda_+ t},$$
$$\lambda_- = \lambda - \frac{i\Delta\omega}{2}, \qquad \lambda_+ = \lambda + \frac{i\Delta\omega}{2},$$

and writing down the characteristic equation as:

$$(\lambda_+ + \delta_1)(\lambda_- + \delta_m) - A = 0, \quad \frac{D_0^2\omega_0^2\omega_1\Lambda}{m\omega_m L^2} = A.$$

The solutions of characteristic equation are:

$$\lambda_{1,2} = -\frac{\delta_1 + \delta_m}{2} \pm \sqrt{\mathrm{Det}},$$
$$\mathrm{Det} = \left(\frac{\delta_1 - \delta_m}{2} - \frac{i\Delta\omega}{2}\right)^2 + A.$$

The condition of instability is the following:

$$\Re\sqrt{\mathrm{Det}} > \frac{\delta_1 + \delta_m}{2}. \tag{84}$$

Using a convenient formula:

$$\mathrm{Det} = a + ib,$$
$$\Re\sqrt{\mathrm{Det}} = \frac{\sqrt{2}}{2}\sqrt{\sqrt{a^2+b^2} + a}.$$

we can rewrite the condition (84) as:

$$\frac{1}{2}\left(\sqrt{a^2+b^2} + a\right) > \left(\frac{\delta_1 + \delta_m}{2}\right)^2, \tag{85}$$

$$a^2 + b^2 = A^2 + \left(\frac{(\delta_1 - \delta_m)^2}{4} + \frac{\Delta\omega^2}{4}\right)^2 + $$
$$+2A\left(\frac{(\delta_1 - \delta_m)^2}{4} - \frac{\Delta\omega^2}{4}\right) \tag{86}$$

Note that for the resonance case ($\Delta\omega = 0$) the solution of (84 or 85) is known: $A > \delta_1\delta_m$. For our case $\delta_m \ll \delta_1$ it means that $A \ll \delta_1^2$. Therefore for small detuning $\Delta\omega \ll \delta_1$ we can expand $a^2 + b^2$ in series in terms of A and rewrite condition (85) as:

$$\begin{aligned}
\frac{1}{2}\left(\sqrt{a^2+b^2}+a\right) &\simeq \frac{A}{2} + \frac{(\delta_1-\delta_m)^2}{4} + \\
&+\frac{A}{2}\,\frac{(\delta_1-\delta_m)^2-\Delta\omega^2}{(\delta_1-\delta_m)^2+\Delta\omega^2} \\
A\frac{(\delta_1-\delta_m)^2}{(\delta_1-\delta_m)^2+\Delta\omega^2} &> \delta_1\delta_m, \\
\text{Or}\quad A &> \delta_1\delta_m \times \frac{(\delta_1-\delta_m)^2+\Delta\omega^2}{(\delta_1-\delta_m)^2}. \qquad (87)
\end{aligned}$$

Let us underline that condition (87) is obtained for small detuning $\Delta\omega \ll \delta_1$. However, considering situation more attentively one can conclude that expansion in series (and consequently the formula (87)) is valid for the condition:

$$A \ll \frac{(\delta_1-\delta_m)^2}{4} + \frac{\Delta\omega^2}{4} \qquad (88)$$

We see that this condition is fulfilled for the solution (87). Therefore we conclude that solution (87) is approximately valid *for any detunings* $\Delta\omega$.

REFERENCES

[1] A. Abramovici *et al.*, *Science* **256**(1992)325.

[2] A. Abramovici *et al.*, *Physics Letters* **A218**, 157 (1996).

[3] Advanced LIGO System Design (LIGO-T010075-00-D), Advanced LIGO System requirements (LIGO-G010242-00), available in http://www.ligo.caltech.edu .

[4] V. B. Braginsky, M. L. Gorodetsky, and S. P. Vyatchanin, *Physics Letters* **A264**, 1 (1999); cond-mat/9912139;

[5] V. B. Braginsky, M. L. Gorodetsky, and S. P. Vyatchanin, *Physics Letters*, **A 271**, 303-307 (2000).

[6] M.Pinard, Z. Hadjar and A. Heidman, http//:xxx.lanl.gov/quant-ph/9901057 (1999).

[7] V. B. Braginsky and I. I. Minakova, Bull. of MSU, ser. III, no.1, 83 (1964).

[8] V. B. Braginsky A. B. Manukin, and M. Yu. Tikhonov, Sov. Phys. JETP **58**, 1550 (1970).

[9] Yu. T. Liu and K. S. Thorne, submited to *Phys. Rev. D.*

[10] V. B. Braginsky, E. d'Ambrosio, R. O'Shaughnessy, S. E. Strigin, K. Thorne, and S. P. Vyatchanin, report on LSC Meeting, Baton Rouge, LA, 16 March 2001, LIGO document G010151-00-R (http//:www.ligo.caltech.edu/).

[11] "Physical acoustics. Principles and Methods." Edited by W. P. Mason, Vol. I, *Methods and devices*,Part A, *Academic press* , New York and London (1964).

[12] Kenji Numata, "Intrinsic losses of various kind of fused silica", proceedings of Forth Edoardo Amaldi Conference, Pert , 2001. (Trancparencies are temporary available in ftp://t-munu.phys.s.u-tokyo.ac.jp/pub/numata/Transparencies/Amaldi/Amaldi4.pdf)

[13] A. Gillespi and F. Raab, *Phys. Rev. D* **52**, 577 (1995).